Top Heterocycl Chem (2014) 33: 143–202
DOI: 10.1007/7081_2013_99

Published online: 19 April 2013

Degradation Pathways for Porphyrinoids

Jacek Wojaczyński

Abstract Porphyrin, a tetrapyrrolic aromatic macrocycle, is relatively resistant to degradation. However, certain strong oxidants (e.g. chromic acid) cause its decomposition to monopyrrolic units. More often, ring opening caused by attack of oxidant on a *meso*-position has been observed. Such degradation by metal salts (thallium(III), cerium(IV)), nitric acid, and other reagents has been studied. Light-driven macrocycle opening by dioxygen has also been noted. Coupled oxidation of metalloporphyrins has been investigated mainly as a mimics of heme degradation observed in vivo.

Modifications of parent porphyrin macrocycle can cause a prominent change of its reactivity toward oxidants. In particular, inversion of one of the pyrrole rings (in N-confused porphyrin) or removal of one of the methine bridges (in corrole) increases macrocycle susceptibility to oxidative ring opening.

Keywords Biliverdin · Coupled oxidation · Degradation · Photooxidation · Tetrapyrrole

Contents

J. Wojaczyński (✉)
Department of Chemistry, University of Wrocław, 14 F. Joliot-Curie St., 50383 Wrocław, Poland
e-mail: jacek.wojaczynski@chem.uni.wroc.pl

Abbreviations

CAN	Cerium(IV) ammonium nitrate
DDQ	2,3-Dichloro-5,6-dicyanobenzoquinone
FCC	Fluorescent chlorophyll catabolite
HO	Heme oxygenase
NBS	*N*-Bromosuccinimide
NCC	Nonfluorescent chlorophyll catabolite
$OEBH_3$	2,3,7,8,12,13,17,18-Octaethylbilindione
$OEPH_2$	2,3,7,8,12,13,17,18-Octaethylporphyrin
$OEPOH_3$	2,3,7,8,12,13,17,18-Octaethyloxophlorin (2,3,7,8,12,13,17,18-octaethyl-5-hydroxyporphyrin)
PDT	Photodynamic therapy
$TPPH_2$	5,10,15,20-Tetraphenylporphyrin
TTFA	Thallium(III) trifluoroacetate
TTN	Thallium(III) nitrate

1 Scope and Limitations

This review is focused on degradation of tetrapyrrolic macrocycles: porphyrins, their N-confused isomers, and corroles (**1**–**3**, Fig. 1). "Degradation" is understood here as a disruption of a macrocyclic system. For this reason, reactions leading only to the lowering of number of rings of the starting pentacyclic system are not included, although formation of secochlorins **4** [1–3] or vacataporphyrins **5** [4, 5] (Fig. 2) also results in a qualitative change of the macrocycle properties. Similarly, processes connected with the loss of the macrocyclic aromaticity without ring opening (e.g. formation of phlorins) will not be discussed unless they serve as a preliminary stage of the actual degradation. Ring-opening reactions of phthalocyanines, porphyrazines, and similar macrocycles as well as systems containing less or more than four pyrrolic

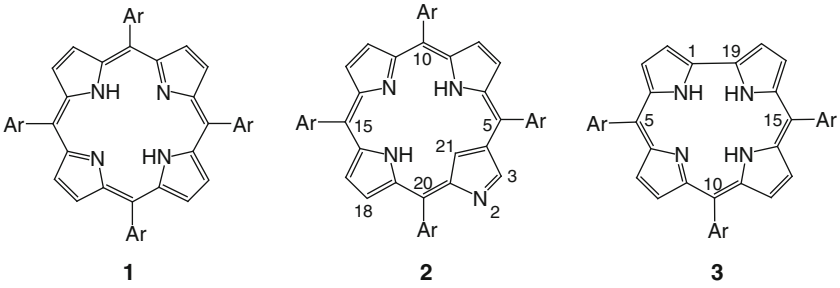

Fig. 1 Porphyrin, its N-confused isomer and corrole (*meso*-aryl derivatives are shown)

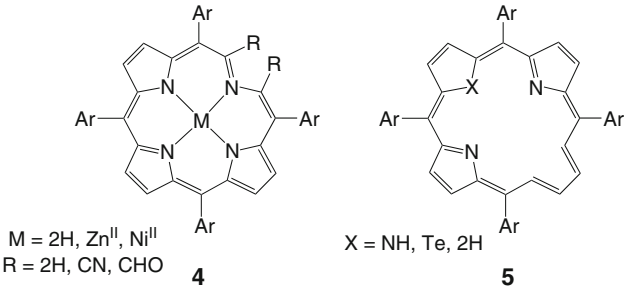

Fig. 2 Examples of secochlorins (**4**) and vacataporphyrins (**5**) [1–5]

rings are not presented. The emphasis is laid on the literature published in the years 2000–2012, but for the sake of comparison, older achievements are also briefly described.

The porphyrin macrocycle containing a conjugated 18 π-electron system is known to be highly stable toward destruction. This fact inspired search for methods of ring opening. The interest in degradation of cyclic tetrapyrroles is connected with several aspects: analytical (structure determination), biochemical (heme and chlorophyll metabolism, formation of algae biliproteins), catalytic (stability of porphyrin derivatives used as catalysts and photosensitizers), and synthetic (preparation of linear oligopyrrolic systems exhibiting interesting properties: helical chirality [6–9], conformational flexibility connected with possible *E–Z* isomerization [10], specific and sometimes unpredictable coordination modes [11–14]).

A direct opening of porphyrin macroring is achieved when one of the C(α)–C (*meso*) bonds is cleft. Reactions at the macrocycle periphery occur preferentially on *meso* positions unless sterical reasons preclude access to this part of molecule [15]. In general, degradation is caused by various oxidants (reduction with hydriodic acid in acetic acid being a notable exception) and is thus preceded by their attack on one of the methine bridges. On the other hand, numerous examples of pyrrole- and metal-centered oxidations have been also described, which can also constitute a preliminary step of further macrocycle decomposition.

This chapter is divided into eight sections. Section 2 is devoted to traditional methods of structure determination based on destruction of tetrapyrrolic systems. In Sect. 3, macrocycle opening by oxidants is discussed, excluding light-driven reactions with dioxygen (Sect. 4) and coupled oxidation of metalloporphyrins (Sect. 5). Biodegradation is shortly presented in Sect. 6, followed by concluding remarks (Sect. 7) and reference list.

2 Degradation Used as Analytical Tool

Classical methods used for structure elucidation of tetrapyrrolic compounds (both cyclic ones and linear derivatives) utilized oxidative degradation with chromic acid, potassium permanganate [16, 17], and ozone [18] or hydriodic acid reduction [19]. Analysis of the resulting monopyrrolic units (maleimides, succinimides) which could be identified, allowed recognition of β-substitution pattern, and in certain cases also *meso* substituents [15]. Among those methods, chromic acid (CrO_3/H_2SO_4) oxidation used in combination with gas chromatography and mass spectrometry has been most widely applied, particularly for identification of chlorophyll derivatives, bilins, and geoporphyrins [20–27]. More recently, this method was used in the analysis of hematoporphyrin derivative used in photodynamic therapy [28, 29]. A new method was described allowing quantitative determination of chlorophyll derivatives by analysis of amount of ethylmethylmaleimide formed during degradation with chromic acid [30].

Formally, part of analytical methods commonly used for the characterization of newly synthesized tetrapyrrolic macrocycles also involves destruction of the molecule. Elementary (combustion) analysis is widely performed, though the results are sometimes not quite satisfactory due to the ease of incorporation of various guest molecules, including solvents, in the crystal lattice of porphyrins [31]. Also a conventional method of carbon isotopic composition of geoporphyrins relies on combustion to CO_2 which is examined by mass spectrometry [32, 33]. Fragmentation observed in certain techniques of mass spectrometry serves as a source of a valuable structural information [34–36]. Analytical data based on other methods involving sample decomposition, such as combustion calorimetry experiments [37, 38], differential scanning calorimetry, and thermogravimetry [39–41] are less frequently reported.

3 Ring Opening by Oxidants

Ring-centered reactions of porphyrin derivatives with various oxidants can lead to opening of the macrocycle without its complete disintegration. Systematic research on oxidation of tetrapyrrolic macrocycles was performed in the 1960–1970s;

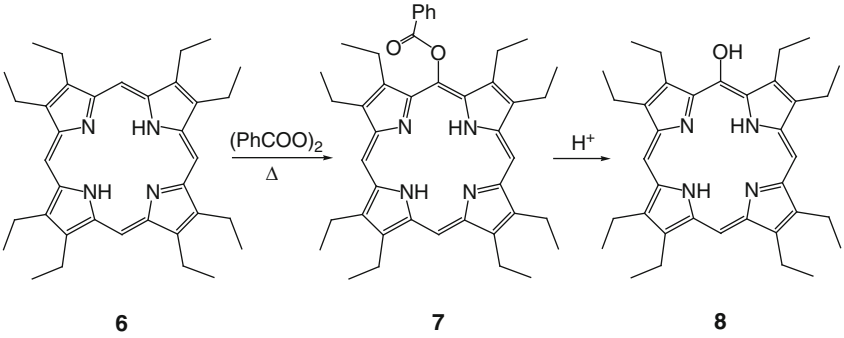

Scheme 1 Synthesis of octaethyloxophlorin [43, 44, 46]

in most of the recent contributions specifically modified systems or reactions conducted under modified conditions have been discussed.

In Sect. 3.1, reactions of porphyrins and their complexes with redox innocent metals are described. Degradation of iron and manganese porphyrin complexes by reagents which are typically used in metalloporphyrin-catalyzed oxidations is discussed in Sect. 3.2. The section is concluded by description of reactivity of N-confused porphyrins and corroles.

3.1 Oxidation of Porphyrins and Their Complexes

Reactions of porphyrins and their complexes with oxidants were extensively studied by Bonnett and coworkers [42–46] and Smith et al. [47–53]. Special attention was devoted to *meso* oxidation leading to oxophlorin (5-hydroxyporphyrin) derivatives due to importance of iron oxophlorins as intermediates in the process of heme degradation. Octaethyloxophlorin ($OEPOH_3$, **8**) was obtained from the reaction of 2,3,7,8,12,13,17,18-octaephylporphyrin ($OEPH_2$, **6**) with benzoyl peroxide [43, 44, 46]. A radical attack at *meso* position gave 5-benzoyloxyporphyrin **7** at ca. 30% yield, and its hydrolysis led to the desired product **8** (Scheme 1). This compound was also prepared by ring synthesis and by coupled oxidation (see 5.1) [43, 44].

Bonnett et al. prepared octaethyloxophlorin **8** by treatment of $(OEP)Fe^{II}(py)_2$ dissolved in pyridine with hydrogen peroxide [43, 45]. Later it was found that reaction did not occur with zinc(II), nickel(II), copper(II), iron(III), and cobalt(III) complexes, while oxophlorins were obtained for Fe(II), Co(II) and Mn(II) or Mn(III) (i.e. metal ions with an easily accessible higher oxidation state) [45]. Conversion of iron(III) oxophlorin into verdoheme analog and its further conversion to biliverdin **9** (Fig. 3) was also described [45].

Kalish et al. demonstrated that treatment of deuteroheme, mesoheme, or protoheme with hydrogen peroxide in pyridine solution yielded all four isomeric oxophlorin complexes in comparable yields [54]. In contrast, oxidation of iron(II)

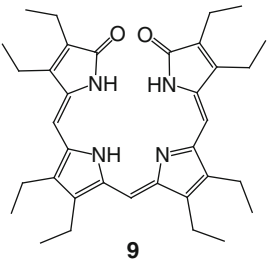

9

Fig. 3 Octaethylbilindione – a synthetic biliverdin analogue

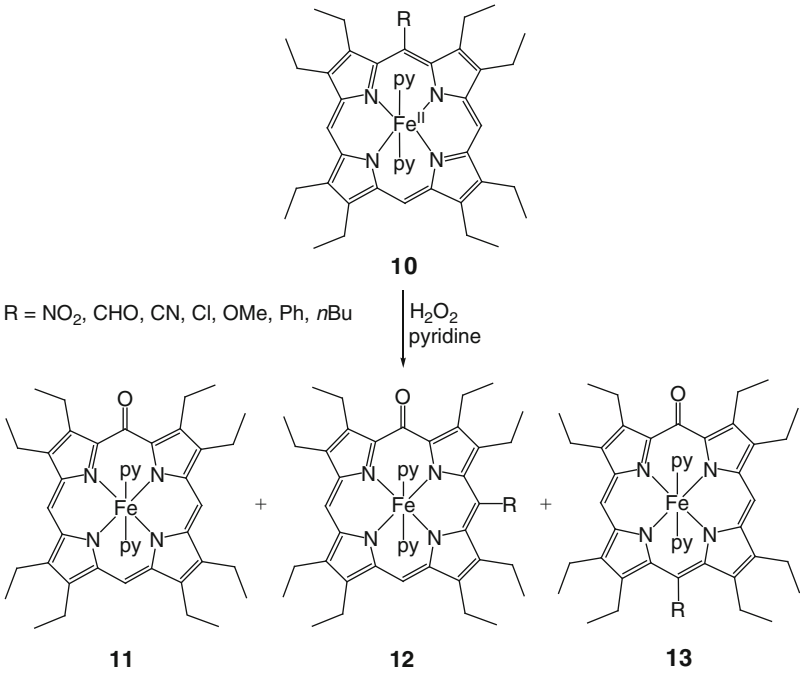

Scheme 2 Oxidation of 5-substituted iron(II) octaethylporphyrins [55]

5-substituted-octaethylporphyrins (5-R-OEP)$Fe^{III}(py)_2$ (R = NO_2, CHO, CN, Cl, OMe, Ph, *n*-Bu) exhibited a strong dependence on the nature of the substituent: yields of (OEPO)$Fe(py)_2$, a product of replacement of R group with oxygen function, varied from 0% (R = Ph, *n*-Bu) to 100% (R = NO_2), while ratio of *cis* to *trans*-oxygenated products (**12** and **13**, Scheme 2) changed from 5.0 (R = CN) to 1.4 (R = Ph) [55].

Treatment of zinc or magnesium complexes of octaethylporphyrin **14** with thallium(III) trifluoroacetate (TTFA) followed by demetallation gave high yields (55–79%) of oxophlorin **8** [49, 50]. 5-Trifluoroacetoxyporphyrins **15** were isolated as stable intermediates of this process (Scheme 3). Similar reactivity was observed when lead(IV) or mercury(II) trifluoroacetates were used, but yields of oxophlorins

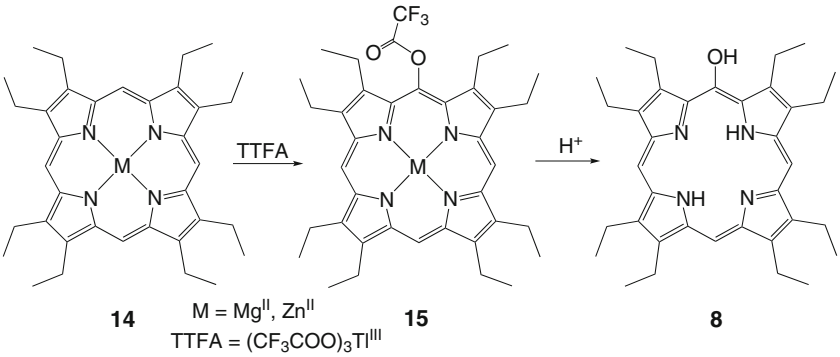

Scheme 3 Oxidation of OEP complexes with TTFA leading to $OEOPOH_3$ [49, 50]

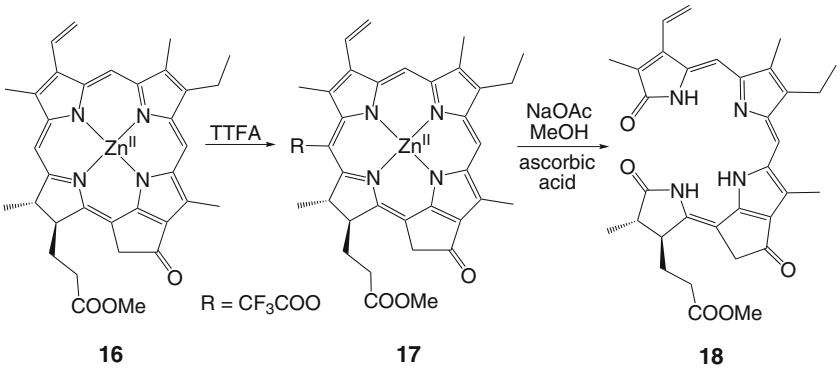

Scheme 4 TTFA oxidation of zinc(II) methyl pyropheophorbide *a* [53]

were significantly lower (19–37%) [50]. Iron(III), copper(II), and nickel(II) complexes of OEP were found resistant to the TTFA attack. An analogous reaction of zinc(II) methyl pyropheophorbide *a* **16** with TTFA, followed by hydrolysis in the presence of ascorbic acid and air proceeded regioselectively to give dihydrobiliverdin **18** (Scheme 4) [53].

In contrast to OEP complexes, zinc tetraphenylporphyrin ((TPP)Zn^{II} **19**) was converted by TTFA, thallium(III) nitrate (TTN) or cerium(IV) ammonium nitrate (CAN) into a ring-opened tetrapyrrole **20** along with 5,15-disubstituted products **21**, **22** (Scheme 5) [51, 52]. These compounds were obtained after acidic workup and chromatography on alumina column. The proper structure of compound **20**, formed by addition of water molecule to the demetallated primary product, was established in the course of studies on photooxidation of TPP complexes (Sect. 4.1).

Interestingly, when zinc(II) 5,10,15-triarylporphyrins were reacted with thallium(III) trifluoroacetate, an oxidative dimerization was observed leading to *meso–meso* linked diporphyrins (Scheme 6) [56]. A similar reactivity of zinc di- and triarylporphyrins with silver(I) salts was reported by Osuka and coworkers [57–59].

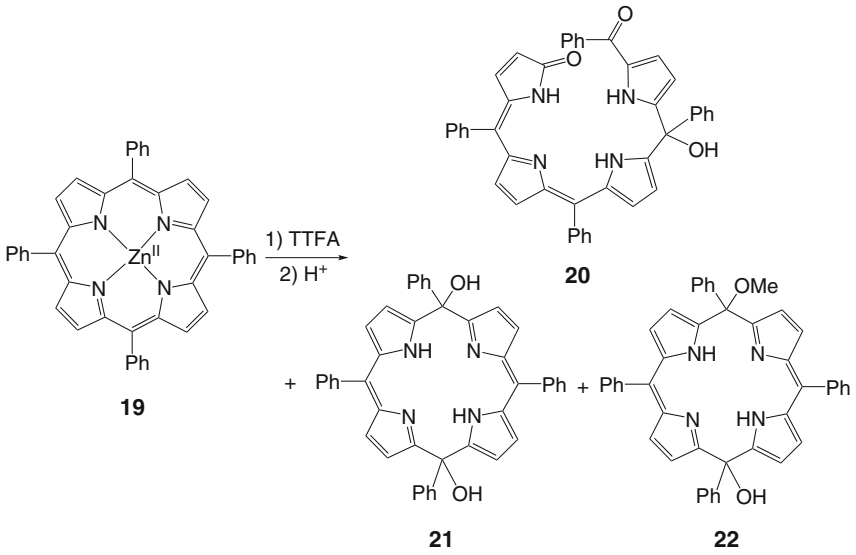

Scheme 5 TTFA oxidation of $(TPP)Zn^{II}$ [51, 52]

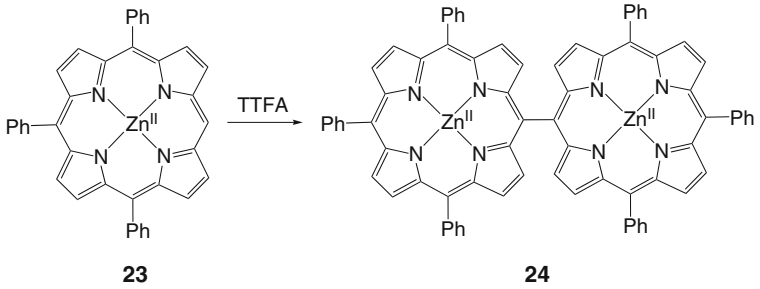

Scheme 6 Dehydrodimerization of zinc(II) triphenylporphyrin [56]

In case of TTN and CAN oxidation of $(TPP)Zn^{II}$, β-nitrated product **25** (Fig. 4) was also isolated [51, 52]. *Meso*-nitration of octaethylporphyrin was reported by Bonnett and Dimsdale, who used fuming nitric acid–acetic acid mixture for this reaction; ring opening was not observed under these conditions [42]. Catalano et al. established the dependence of the site of reaction with nitrogen dioxide on the metal coordinated to tetraphenylporphyrin [60]. Nickel(II), copper(II), and palladium(II) complexes were exclusively converted to 2-nitro derivatives, while for more electropositive zinc(II) and magnesium(II) ions ring opening resulting from the reaction at *meso* position was noted. This observation was rationalized by a different symmetry of π-cation radicals formed by oxidation of metalloporphyrin with NO_2. Also reaction of $(TPP^{+\bullet})Zn^{II}(ClO_4)$ with various nucleophiles yielded mainly 2-substituted derivatives, but in the particular case of nitrite anion,

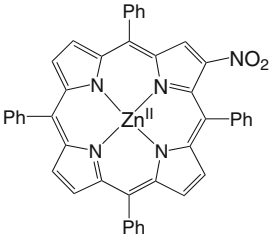

25

Fig. 4 Zinc 2-nitro-5,10,15,20-tetraphenylporphyrin

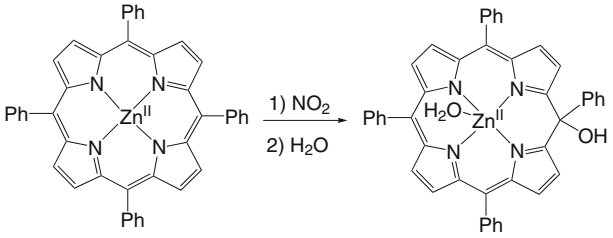

19 **26**

Scheme 7 Formation of zinc(II) isoporphyrin [63]

β-nitrated porphyrin product was accompanied with an open-chain compound **20** [61]. More recently, Sarkar et al. described a formation of *meso*-hydroxylated isoporphyrin **26** upon treatment of *meso*-tetrakis(3,4,5-trimethoxyphenyl)porphyrin iron(III) or zinc complex with NO_2 (O_2 and NO, Scheme 7) [62, 63]. Further degradation of iron isoporphyrin in solution was observed, and formation of verdoheme- and biliverdin-type products was postulated on the basis of UV–vis spectra. In contrast, zinc derivative remained stable in presence of air and light.

Oxidation of macrocycle can be facilitated by an appropriate modification of the porphyrin ring (both sterical aspects and generation of specific reactivity by substitution are of importance). Ring opening of sterically hindered, dodecasubstituted porphyrins **27** via $NaNO_2$ treatment in the presence of trifluoroacetic acid and air was studied by Ongayi et al. [64–66]. Authors attributed the ease of degradation of porphyrinic substrates **27** to the tendency to relieve steric strain. The proposed reaction pathway involved oxidation of macrocycle by NO^+ to a π-cation radical followed by ring opening by dioxygen. A primary bilitrienone product **29** was isolated in 70% yield (Scheme 8), but only for nonyl-substituted system, while in case of *meso*-tetraphenyl derivative the unstable compound **29** was converted to a biladienone **31** by addition of water. Two isomers of hydrated benzoylbiliverdin **31** were separated, presumably differing in the configuration of C(4)–C(5) bond. Hydration of nonyl derivative **29** was observed as well, but it could be inverted by heating the product **31** above 40°C [66].

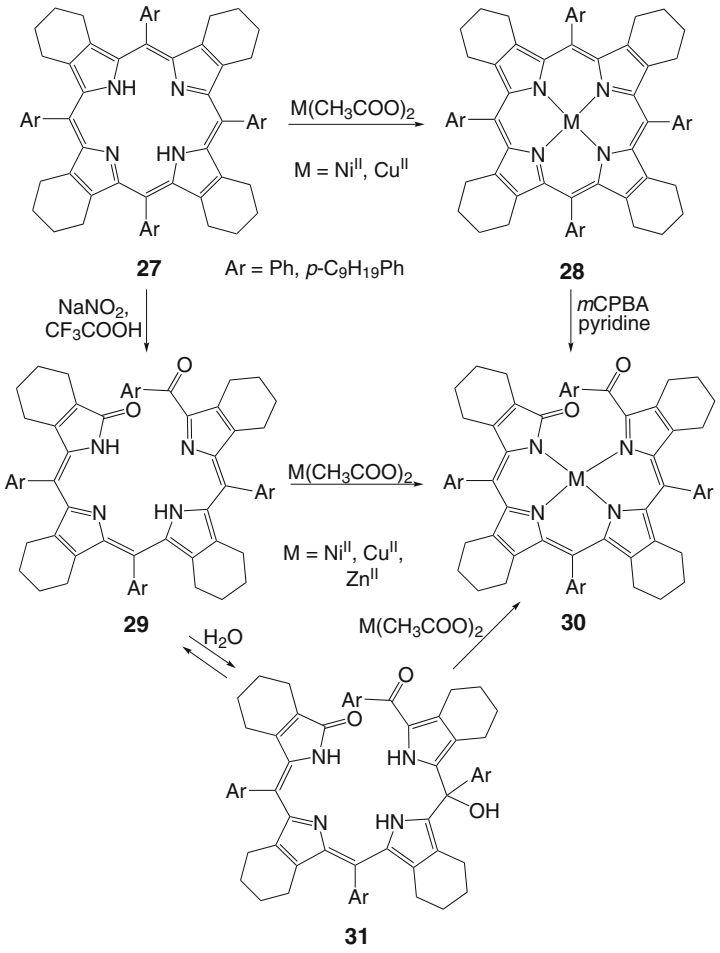

Scheme 8 Degradation of dodecasubstituted porphyrins [64–66]

Metallation of **31** with Ni(II), Cu(II), and Zn(II) ions led to formation of 4N chelates **30** in which a dehydrated form of tetrapyrrole was found [65]. Nickel(II) and copper(II) complexes were also prepared by an alternative route from the corresponding metalloporphyrins **28** which were oxidized using *meta*-chloroperoxybenzoic acid in pyridine in the presence of air (Scheme 8) [65].

Yashunsky, Morozova, and Ponomarev described a conversion of nickel complexes of 5-formylporphyrin oximes **32** in a mixed water-organic solvent system into brown-yellow products [67, 68]. These products were identified as open-chain tripyrroryloxazoles **33** and were isolated by column chromatography in ca. 50% yield (Scheme 9) [68]. A mechanism was proposed involving conversion of oxime substituent into 1,2-oxazine ring and oxidation of formed intermediates by dioxygen leading to fission of pyrrolic β,β′ bond and elimination of α-carbon.

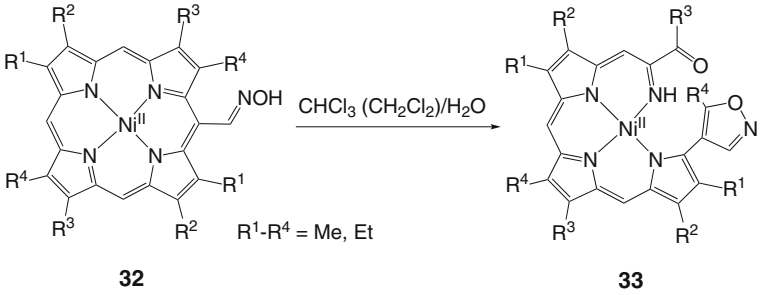

Scheme 9 Conversion of 5-formylporphyrin oximes to tripyrroryloxazoles [67, 68]

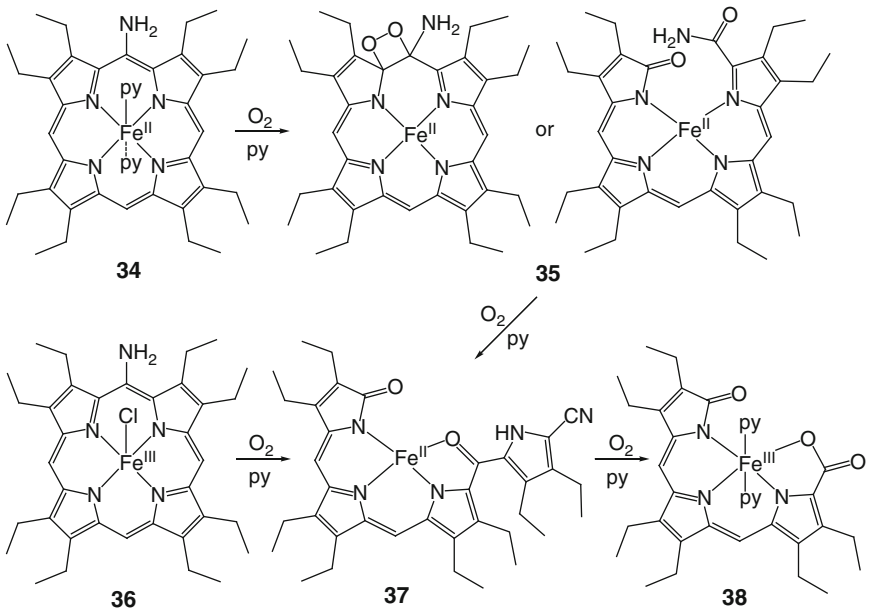

Scheme 10 Ring opening of iron *meso*-aminoporphyrin complexes [69, 70]

A remarkable ease of ring opening was observed for *meso*-amino-substituted octaethylporphyrin complexes, $(H_2N\text{-OEP})Fe^{II}(py)_2$ **34** and $(H_2N\text{-OEP})Fe^{III}Cl$ **36** [69, 70]. The exposure of their pyridine solutions to dioxygen resulted in its regioselective attack at the substituted carbon; ring opening was followed by a second oxidation step introducing another *meso*-oxygen atom; at the same time the terminal amide fragment was dehydrated to cyano group (Scheme 10). A resulting (3N + O) complex **37** and its analog with an axial ethanol ligand were characterized by X-ray crystallography. In the case of **34** oxidation, a green

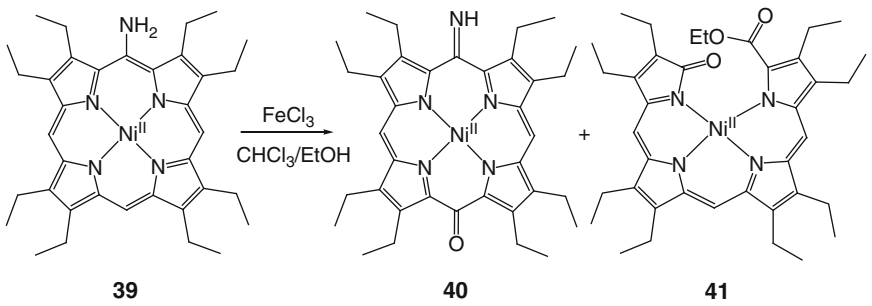

Scheme 11 Oxidation of nickel(II) *meso*-aminoporphyrin

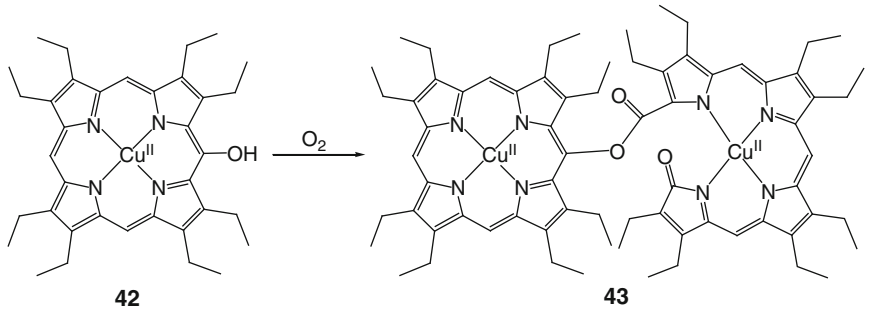

Scheme 12 Formation of dinuclear copper complex [14]

intermediate was detected [69]. Its ^{1}H NMR spectrum indicated a significant degree of ligand radical character and symmetry lowering with respect to the starting iron (II) complex **34**, which was attributed to the formation of dioxygen adduct or iron biliverdin derivative **35**. A prolonged contact with dioxygen resulted in a slow conversion of compound **37** to a mixture of tripyrrole complex **38** and small amounts of another unidentified product [70].

A pyridine solution of nickel(II) complex of 5-aminooctaethylporphyrin **39** remained unchanged upon exposure to dioxygen [71]. A slow reaction was observed, however, when iron(III) chloride was used as oxidant (Scheme 11), yielding a biliverdin derivative **41** as a minor isolated product (10% yield).

Phillips et al. reported an oxidative ring opening of copper oxophlorin complex **42** yielding an ester-linked, dinuclear copper complex **43** (Scheme 12) [14]. A proposed mechanism included oxidation of macrocycle by dioxygen leading to (OEPO$^{\bullet}$)Cu^{II} complex, its reaction with the starting (OEPOH)Cu^{II} to produce a C–O link, ring opening by addition of dioxygen and termination of the process by superoxide anion.

A formation of verdoheme analog **45**, which was further hydrolyzed to octaalkylbiliverdin **46**, was observed by Chang et al. upon oxygenation of cobalt(II) porphyrin substituted with naphthoic acid **44** (Scheme 13) [72]. The substituent was believed to support the activation of molecular oxygen by the metal center and was finally cleft

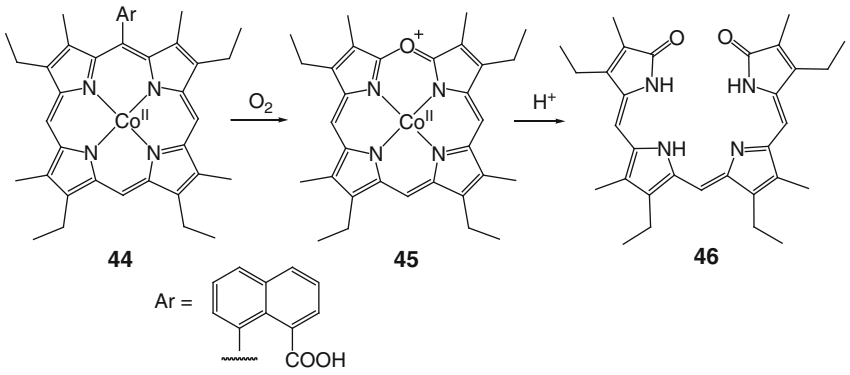

Scheme 13 Oxygenation of cobalt(II) porphyrin substituted with naphthoic acid [72]

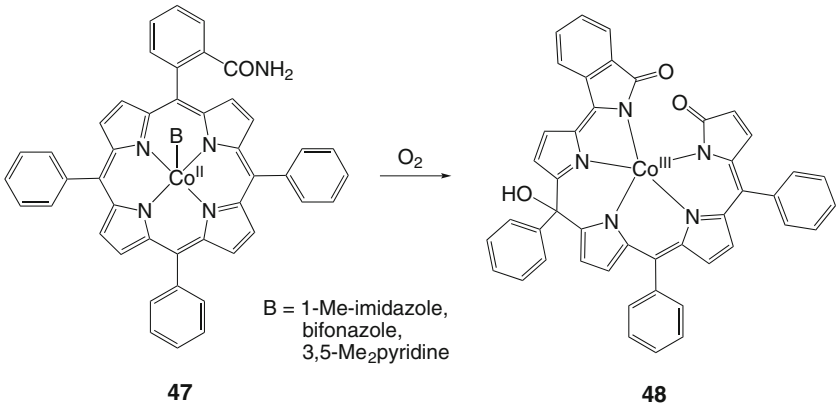

Scheme 14 Formation of Co(III) complex of an acyclic penatpyrrole [73]

as 8-formyl-1-naphthalenecarboxylic acid. A helical cobalt(III) complex of acyclic pentapyrrole **48** was obtained by Yamanishi et al. by treatment of cobalt(II) 5-(2-carbamoylphenyl)-10,15,20-triphenylporphyrin **47** with 1-methylimidazole and air (Scheme 14) [73]. An amide substituent and axial base (imidazole and pyridine derivatives were tested) was found essential for dioxygen activation, which resulted in breaking in C(4)–C(5) bond, followed by formation of oxoisoindole ring and addition of hydroxyl group to a *meso* position. Chiral HPLC separation of racemic **48** was performed. The application of chiral axial ligands bearing (*S*) configuration: nicotine, cotinine, or bifonazole led to the preferential formation of (*M*)-helical form of pentapyrrolic product.

An unexpected ring opening upon bromination of tetraphenylporphyrin with 20 equivalents of *N*-bromosuccinimide (NBS) in chloroform–methanol solution was described by Liu et al. [74]. From a mixture of reaction products which was treated with zinc acetate, crystals of compound **50** were isolated (Scheme 15). An X-ray

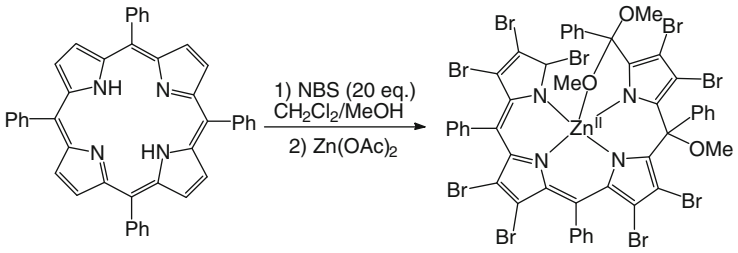

49 **50**

Scheme 15 Ring opening upon bromination of $TPPH_2$ [74]

structure of this zinc complex revealed the presence of nine bromo substituents at pyrrole rings and three methoxy groups attached to *meso* positions. Various *para*-phenyl-substituted tetraarylporphyrins could also be converted to the corresponding ring-opened products formed in 11–46% yield; also zinc tetraphenylporphyrin underwent a similar reaction, while the use of copper(II) and nickel(II) as central ions resulted only in β-bromination. A mechanism of the transformation was proposed involving MeOBr (formed from NBS and methanol) as an active species responsible for perbromination of pyrrole rings to form a highly congested dodecasubstituted macrocycle. The steric hindrance could be released by addition of another MeOBr molecule to C(*meso*)–C(α) bond followed by nucleophillic addition of methoxide to the *meso* positions of ring-opened product.

3.2 Degradation of Metalloporphyrin Catalysts

In this part, we shall discuss reactions of iron and manganese complexes with reagents which are typically used in metalloporphyrin-catalyzed oxidations (hydroxylations, epoxydations): peroxides, peroxyacids, and molecular oxygen [75–78]. Since typically an organic substrate is used in an excess in these processes, the problem of catalyst stability under such conditions has been often neglected. If this has been taken into account, methods of increasing metalloporphyrin robustness have been sought, mainly via its appropriate modification [79–81]. It was achieved by a substitution of porphyrin ring increasing catalytical activity and/or providing steric protection not only against formation of μ-oxo dimer $PFe^{III}–O–Fe^{III}P$ but also against attack of oxidants on *meso* positions [75]. Possible inter- and intramolecular processes leading to degradation of metalloporphyrin have been addressed [82, 83], though papers devoted to the analysis of catalyst stability have been relatively rare [84, 85].

In the recent years, several groups concentrated their efforts on the analysis of oxidation of porphyrin complexes by different oxidants used for the metalloporphyrin-catalyzed oxidations of organic substrates. Starting from simple,

rather qualitative observations of possible decomposition of macrocycle as indicated by intensity lowering of Soret band in the UV–vis spectra, the studies have been typically extended to the analysis of reaction kinetics and attempts of determination of possible reaction mechanisms. However, in most cases the fate of catalyst and structures of degradation products have not been considered.

Stephenson and Bell investigated mechanism and kinetics of iron porphyrin-catalyzed epoxidation of olefins by hydrogen peroxide [86, 87]. Among factors affecting the activity of catalyst, oxidative degradation of porphyrin ring and μ-oxo dimer formation were discussed. The authors attributed the macrocycle decomposition to the attack of hydroxyl radicals (generated from of coordinated hydrogen peroxide). This hypothesis was in agreement with the observation that factors increasing the rate of hydroxyl radical generation contributed also to porphyrin degradation. The efficiency of iron porphyrin epoxidation catalysts was also studied by Cunningham and coworkers [88–90]. They connected the observed bleaching of the catalyst with its direct oxidation in the resting state (Fe(III)) rather than the high-valent intermediates.

Rocha Gonsalves and coworkers analyzed the epoxidation of alkenes by peroxides catalyzed by manganese porphyrins [91]. Two mechanisms of degradation of catalysts were found, depending on their structure and reaction conditions: an intramolecular pathway predominated when a metallo-oxo species was an active intermediate, while a metalloacylperoxo derivative favored an intermolecular one.

Ungvarai-Nagy and coworkers reacted iron(III) complexes of protoporphyrin IX and tetra(4-sulfonatophenyl)porphyrin with bromate and observed macrocycle degradation in acidic solutions [92–94]. Türk et al. investigated the stability of water-soluble porphyrins and their manganese(III) complexes toward peroxides and sodium hypochlorite [95–98]. The degradation rate constants were found dependent on the structure of porphyrin substrate, nature of oxidant, and pH of the solution. However, possible degradation pathways and structures of products formed were not discussed. Lente and Fábián studied kinetics and mechanism of oxidation of water-soluble porphyrin **51** with hydrogen peroxide and peroxomonosulfate anion [99]. The analysis of ESI mass spectra of the reaction mixture revealed the presence of iron complex of biliverdin-type tetrapyrrole **52** and a sulfonated benzoic acid **53** as dominant products of porphyrin decomposition (Scheme 16). Hopefully, this precedent will prompt further works on structural characterization of ring-opened oligopyrroles produced in the course of degradation of metalloporphyrin catalysts.

3.3 Oxidation of N-Confused Porphyrins

Though N-confused porphyrins have been known for almost two decades [100, 101], relative little studies have been devoted to their degradation. However, the instability of these macrocycles during metallation performed under aerobic conditions has been frequently observed. This led Furuta et al. to investigate the nature of the degradation product [102]. They found that in the course of reaction with copper(II) acetate in the

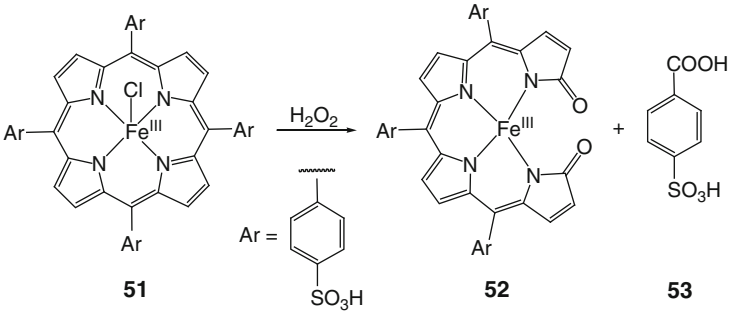

Scheme 16 Degradation of water-soluble iron porphyrin catalyst [99]

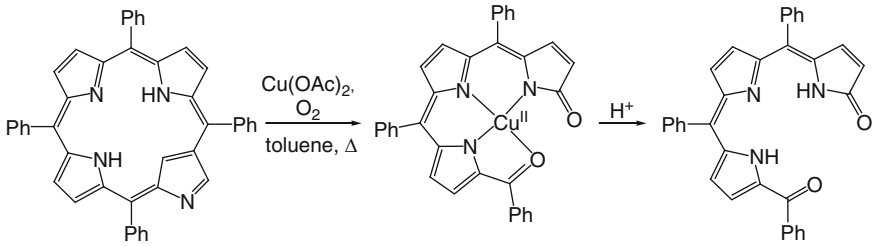

Scheme 17 Degradation of N-confused porphyrin [102]

presence of air N-confused tetraphenylporphyrin **54** underwent an oxidative transformation. Copper(II) complex of a linear tripyrrole **55** was isolated from the reaction mixture in 34% yield (Scheme 17). No other products were identified. Free tripyrrinone **56** and its zinc(II), nickel(II), palladium(II), platinum(II), and cobalt(II) derivatives were obtained [102]; crystal structures of Cu(II) and Pd(II) complexes showed a square-planar, N_3O-coordination mode [103].

A suggested mechanism of the degradation involved two successive reactions with molecular oxygen, activated by coordinated Cu(II) ion, leading to scission of two C(*meso*)–C(α) bonds. Further studies on the regioselectivity of the process, performed on 5-(2-pyridyl) derivative, showed that the N-confused pyrrole was cleft together with 5-aryl substituent, which proved the primary attack of dioxygen at C(1)–C(20) bond [102]. In contrast to this observation, Pawlicki et al. found that copper(II) complex of pyrrole-appended O-confused tetraaryloxaporphyrin **57** reacted with dioxygen yielding both possible tripyrrolic degradation products **58**, **59** (resulting from breaking of either C(1)–C(20) or C(4)–C(5) bond) formed in 7:3 ratio, along with and the product of oxygen atom insertion into a copper–carbon bond **60** (Scheme 18) [104]. Apparently, *meso*- and pyrrole substitution can direct the attack of dioxygen molecule; a discussion on the regioselectivity of oxidative ring opening of N-confused porphyrin can be found in the part devoted to photooxidation of tetrapyrroles (Sect. 4.1).

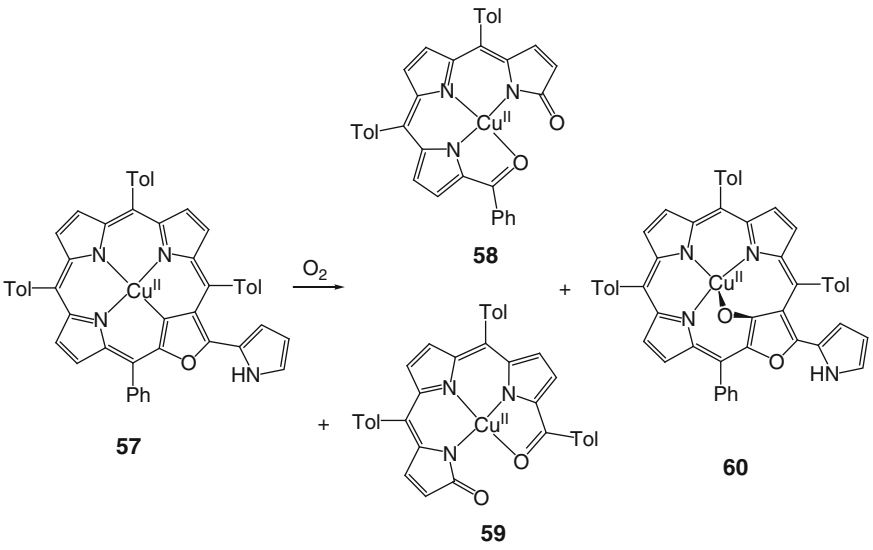

Scheme 18 Oxygenation of copper(II) complex of pyrrole-appended O-confused oxaporphyrin

3.4 Oxidation of Corroles

Despite general similarity to porphyrins, corroles exhibit a specific and sometimes unpredictable reactivity [105]. Both macrocycle families share a common 18-π-electron system, but lack of one *meso* bridge in corroles leads to increase of electron density and, as a consequence, a susceptibility to oxidative ring opening. Interestingly, all reports on such reactions concern *meso*-substituted systems [105], though any systematic and comprehensive research on factors influencing corrole stability has not been performed. Most work in the field concentrated on photooxidation of corroles (see Sect. 4.2). Macrocycle opening by certain oxidants has been also described, though typically formation of biliverdin-type compounds only accompanied the reaction of major interest.

A fully brominated open-chain tetrapyrrole **61** (Fig. 5) was identified as a reaction by-product resulting from breaking of C(4)–C(5) bond of germanium(IV) 5,10,15-triphenylcorrole treated with bromine [106]. A linear tetrapyrrole **62** was formed in minor quantities when triarylcorroles were reacted with 4-amino-4*H*-1,2,4-triazole [107]. This time, C(5)–C(6) bond of the original macrocycle was cut (Fig. 5). Ring opening at C(10) was observed upon conversion of triarylcorrole **63** to a corresponding porphyrin (Scheme 19) [108]. A proposed mechanism of the transformation involved a [2 + 2] cycloaddition of two corroles and cleaving of a spirocyclobutane intermediate by dioxygen connected with an extrusion of *meso*-carbon bearing *para*-nitrophenyl substituent.

Other pathways of corrole oxidation were reported, including isocorrole formation by 2,3-dichloro-5,6-dicyanobenzoquinone (DDQ) treatment [109, 110] or demetallation [111, 112] and oxidative dimerization of 5,10,15-tris(pentafluorophenyl)corrole with formation of β-β′ bond(s) upon heating in 1,2,4-trichlorobenzene [113].

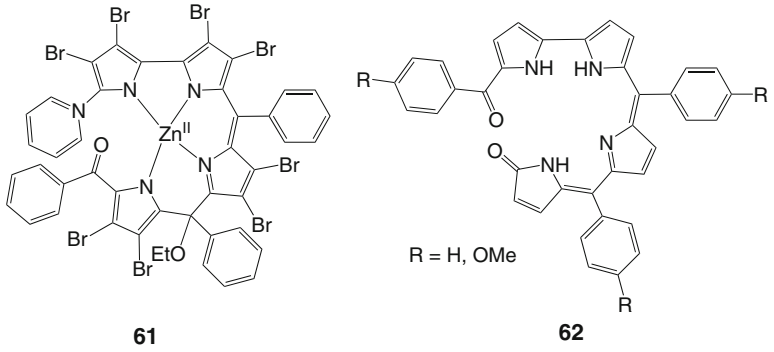

Fig. 5 Ring-opened products of corrole oxidation [106, 107]

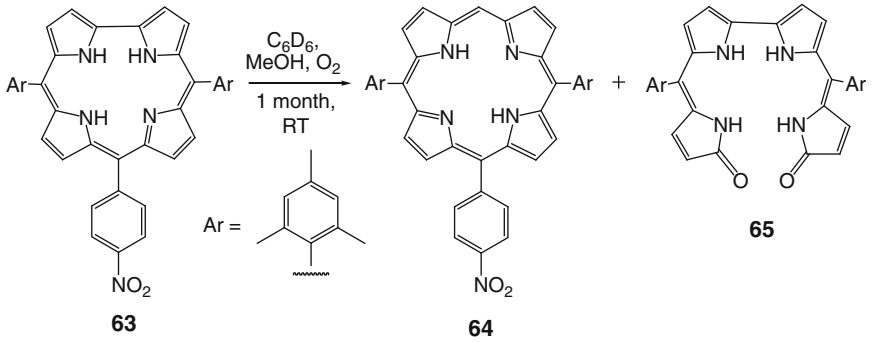

Scheme 19 Conversion of triarylcorrole to poprhyrin and a linear tetrapyrrole [108]

4 Photooxidation of Tetrapyrroles

Photooxidation of tetrapyrrolic macrocycles and their complexes is considered as the most important process responsible for the frequently observed photobleaching of these compounds [114]. This phenomenon is connected with the ability of porphyrin derivatives to activate molecular oxygen in the presence of light. Energy transfer from the excited state of the macrocycle to the ground state of the dioxygen molecule results in the generation of singlet oxygen. As a practical consequence, tetrapyrroles are used as photosensitizers for degradation of various organic substrates [115–117] and in photodynamic therapy (PDT) for treatment of cancer, macular degeneration, chronic skin diseases, and other conditions [118–121]. Under certain conditions, also tetrapyrrole itself can be attacked by singlet oxygen, which may eventually lead to ring opening.

In the context of not only photosensitizer stability but also other applications of tetrapyrroles, light-driven reactivity of porphyrin derivatives toward O_2 is of particular interest. Photobleaching of photosensitizers used in photodynamic

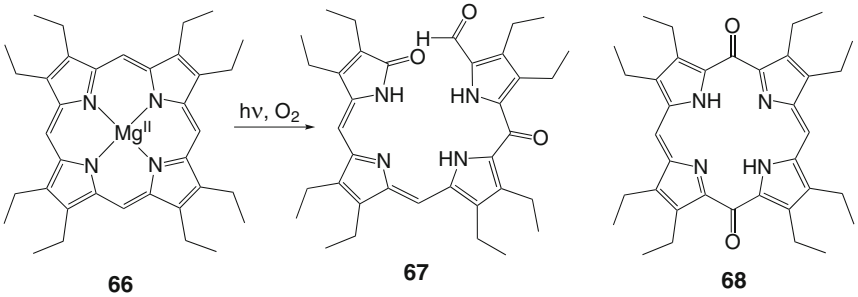

Scheme 20 Photooxidation of (OEP)Mg^{II} [122]. Compounds **67** and **68** were found among products of light-driven oxidation of oxophlorin [123]

therapy was thoroughly reviewed by Bonnett and Martínez [114]. Thus, older contributions will be only briefly described in his chapter, and the attention will be focused on recent developments in the field.

4.1 Photooxidation of Porphyrins, N-Confused Porphyrins and Phlorins

Most metal-free porphyrins are not prone to photooxidative degradation due to the relative high value of oxidation potential. However, their deprotonation or conversion to complexes of electropositive metal ions (e.g. with Zn(II), Cd(II) or Mg(II)) lowers redox potential and therefore the robustness of the system toward oxidative degradation is also reduced.

Fuhrhop and Mauzerall reported the photooxidation of magnesium(II) octaethylporphyrin **66** and identified a linear tetrapyrrole **67** as the final product for this transformation (Scheme 20) [122]. This compound was also found by Bonnett et al. as one of the two main products of photooxidation of octaethyloxophlorin **8** in neutral solution (the other being 5,15-dioxoderivative **68**, Scheme 20) [123]. Light-driven ring opening of zinc, magnesium, cadmium, thallium(I) complexes of tetraphenylporphyrin **69** as well as the porphyrin dianion (TPP^{2-}) was examined by several groups [124–128]. A proper structure of the final product **20** or **70** was finally established by Cavaleiro and coworkers [128]. A bilindione derivative bearing –OR substituent in 15-position resulted from dioxygen attack on the C(*meso*)–C(α) bond, followed by demetallation and addition of water or alcohol (ROH, Scheme 21). As proved by isotope labeling studies, both carbonyl oxygen atoms are derived from the single molecule of O_2 [125, 126]. Silva et al. studied effects of substitution of tetraarylporphyrin on the degradation of cadmium(II) complexes and showed that the reaction was governed by steric factors rather than electronic ones [129]. The presence of substituents in *ortho* positions of phenyl rings prevented the macrocycle from the dioxygen attack (Scheme 22).

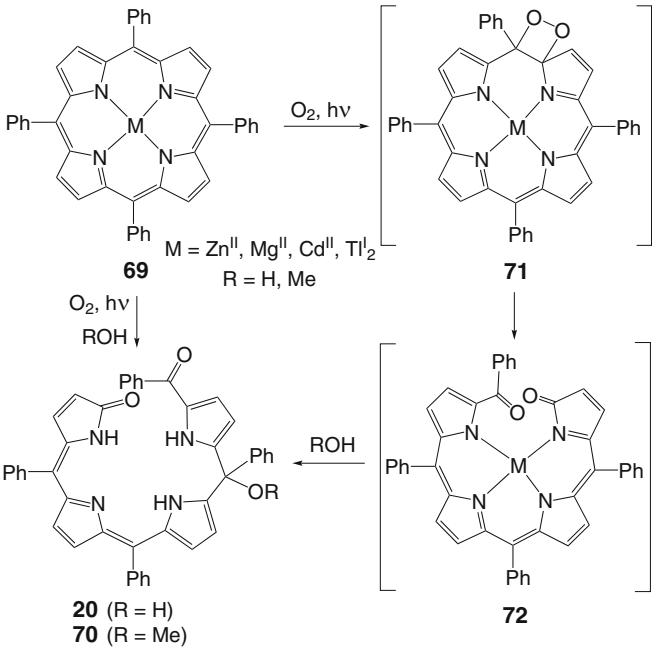

Scheme 21 Photooxidation of TPP complexes [128]

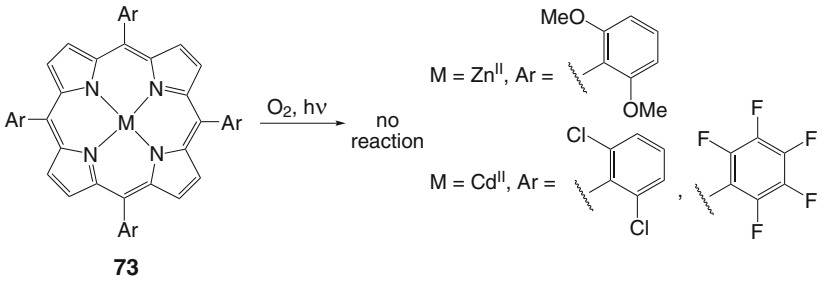

Scheme 22 Zinc(II) and cadmium(II) tetraarylporphyrins not prone to photooxidation [129]

Both cadmium(II) tetra(3,4,5-trimethoxyphenyl)porphyrin **74** and zinc(II) 2,3,12,13-tetrabromoporphyrin **77**, however, were converted to the corresponding open-chain products **75**, **76** (two forms were observed) and **78**, respectively (Schemes 23, 24).

Zinc(II) complexes of linear tetrapyrrole **20** were obtained [130]. Depending on metallation conditions, 3N + O or 4N coordination was found in these chelates, in the latter the loss of methanol or water led to a fully conjugated structure (Scheme 25). Copper(II) complex, formed by transmetallation of photooxidation product of magnesium(II) tetraphenylporphyrin, heated with excess of copper(II) acetate yielded a dinuclear species **82** (Fig. 6); the additional *meso*-oxygen bridging two copper ions originated probably from water since compound **82** was obtained also under dioxygen-free conditions [12].

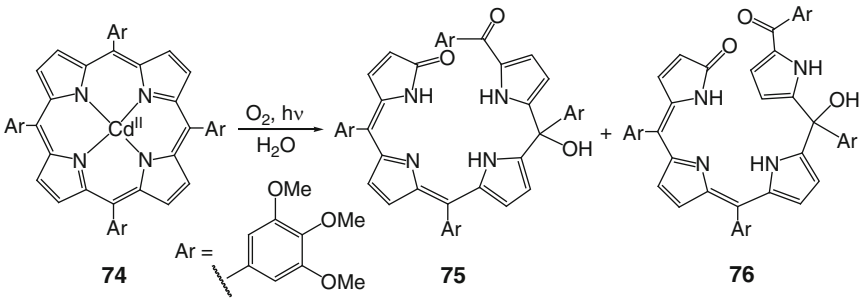

Scheme 23 Photooxidation of cadmium(II) tetra(3,4,5-trimethoxyphenyl)porphyrin [129]

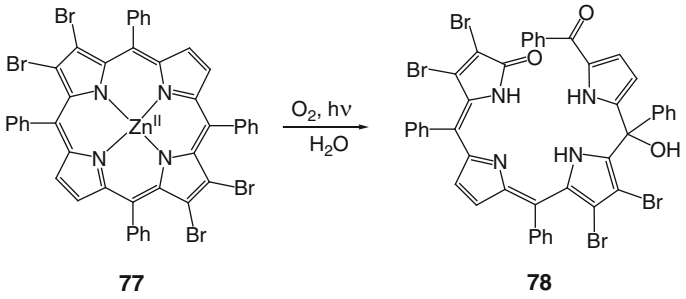

Scheme 24 Photooxidation of zinc(II) β-tetrabromoporphyrin [129]

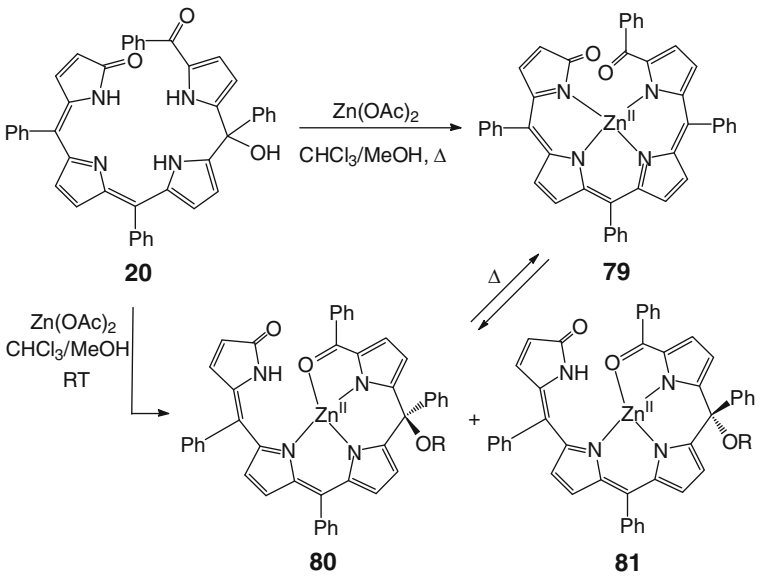

Scheme 25 Metallation of bilindione **20** [130]

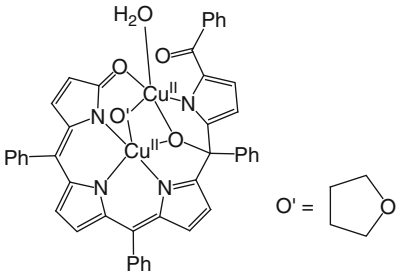

82

Fig. 6 Dinuclear Cu(II) complex

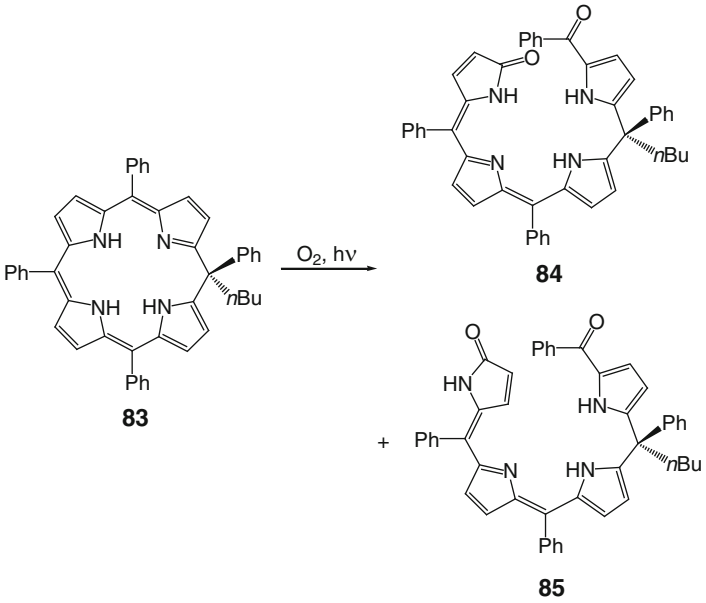

Scheme 26 Photooxidation of *meso*-substituted phlorin [131]

Mixed 3N + O copper(II), nickel(II), and zinc(II) complexes were formed from ligands **84** and **85**, obtained by the photooxidation of a *meso*-substituted phlorin **83** [131]. Two isomers of bilindione and its complexes were described, with a different orientation of the terminal pyrrolone ring (Scheme 26). Their interconversion upon irradiation which caused *E–Z* isomerization was demonstrated. LeSaulnier et al. investigated photodegradation of phlorins bearing different number of mesityl substituents **86** (Fig. 7) [132]. As expected, the incorporation of bulky mesityl substituents enhanced phlorin stability.

Photobleaching of certain metal-free porphyrins was also observed, not necessarily connected with ring-opening reactions. Water-soluble, cationic 5,10,15,20-tetrakis(1-pentyl-4-pyridyl)porphyrin underwent fast photodegradation in aqueous media [133].

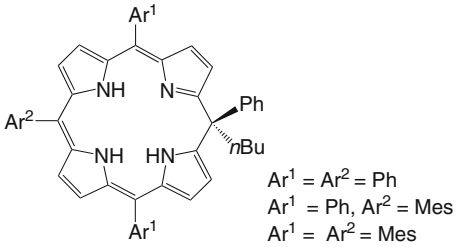

86

Fig. 7 Mesityl-substituted phlorins

Niziolek and coworkers observed that lipid peroxidation in membranes, mediated by protoporphyrin IX as a singlet oxygen photosensitizer, can be prolonged in the presence of nitric oxide [134]. NO was found to protect the macrocycle against oxidative destruction. Cavaleiro et al. carried out photochemical studies on stability of porphyrins and their copper(II) complexes and showed that the latter had shorter triplet lifetimes and were more stable with respect to photodegradation than the respective free bases [135]. Similarly, perfluorination of phenyl substituents of tetraphenylporphyrin had a beneficial effect on the macrocycle robustness.

When 2-aza-21-carba-5,10,15,20-tetraphenylporphyrin (inverted porphyrin **54**) was dissolved in dichloromethane and irradiated with visible light in the presence of air, only traces of degradation products could be detected. Instead, photooxidation of the dianion of N-confused tetraphenylporphyrin **87** was performed which led to a mixture of linear oligopyrroles within 1 h [136]. Chromatographic separation yielded fractions containing tripyrrinone **56** (33% of reacted substrate), its dimethyl acetal **88** (24%) and N-confused tetrapyrrole **89** (31%, Scheme 27). Upon metallation with palladium(II), compound **89** converted into complex **90** containing a conjugated N-confused biliverdin analog acting as a binucleating ligand with two types of coordination surroundings: (NNNO) and (CNOO) (Scheme 27) [136]. Further exploration of photooxidation products led to detection of the additional, unexpected tetrapyrrolic compound **70** (present in ca. 6–9% yield), typically formed in the course of TPP^{2-} degradation [137]. This observation led to a conclusion that two different mechanisms operate in one molecule. Apart from 1,2-dioxygen addition, which is common for tetrapyrrolic macrocycles, the rare 1,3-addition was also found (Scheme 28).

Compound **89**, the major isolated tetrapyrrolic product of photooxidation of N-confused porphyrin dianion resulted from cleavage of C(10)–C(11) bond of the original macrocycle. However, changing of reaction conditions (metallation with zinc or replacing of methoxide with ethoxide for the conversion of N-confused porphyrin to its dianion) allowed us to detect other tetrapyrrolic degradation products (Wojaczyński J, Popiel M, Gońka E, Latos-Grażyński L, unpublished results). DFT calculations performed on inverted porphyrin dianion did not show any significant differences among *meso* positions which could be responsible for any preference of dioxygen attack. Apparently, the observed product distribution reflects not only the regioselectivity of O_2 addition but also the relative stability of

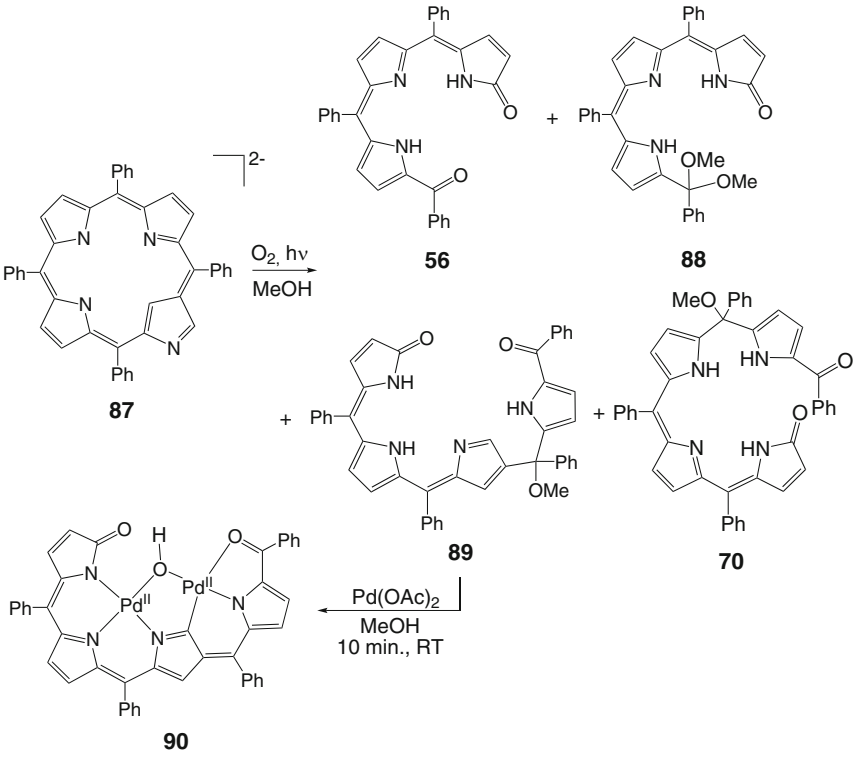

Scheme 27 Photooxiadtion of dianion of N-confused porphyrin and formation of dinuclear palladium complex of N-confused biliverdin derivative [136]

degradation products under given conditions since part of them can undergo further reactions (as proved by the observation of tripyrrinone products **56**, **88** which could be formed from primary ring opening at C(5) or C(20) followed by loss of inverted pyrrole in the second oxidation step).

4.2 Photooxidation of Corroles

The question of photochemical stability of corroles is particularly important in context of their possible application in photoactive devices, chromophores for light energy conversion and singlet oxygen generation [138–140]. Early observations indicated a stepwise degradation of corroles in solution in the presence of light and air. The process was monitored by UV–vis spectroscopy since a systematic lowering of Soret band intensity was observed [141, 142]. The presence of electron-withdrawing substituents in corrole ring or complexation with metal ion was shown to increase the macrocycle robustness. The first proposal of a structure of

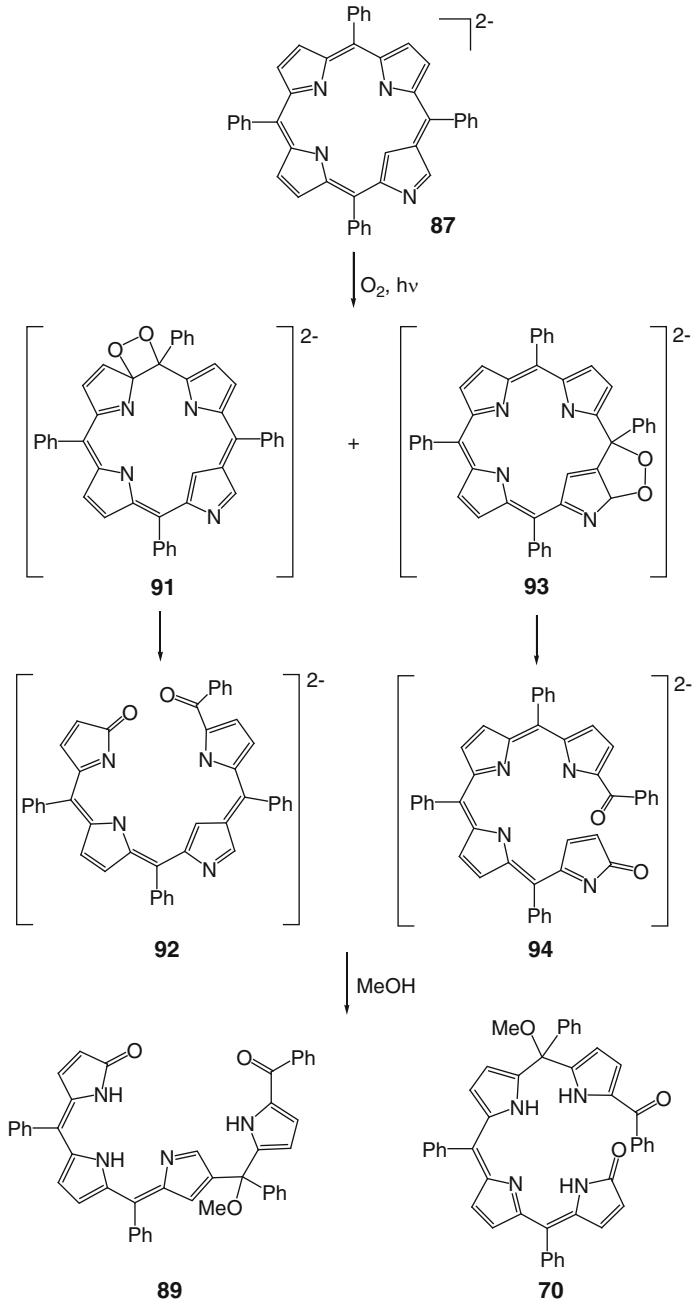

Scheme 28 Mechanism of 1,2- and 1,3-dioxygen addition to dianion **87** [137]

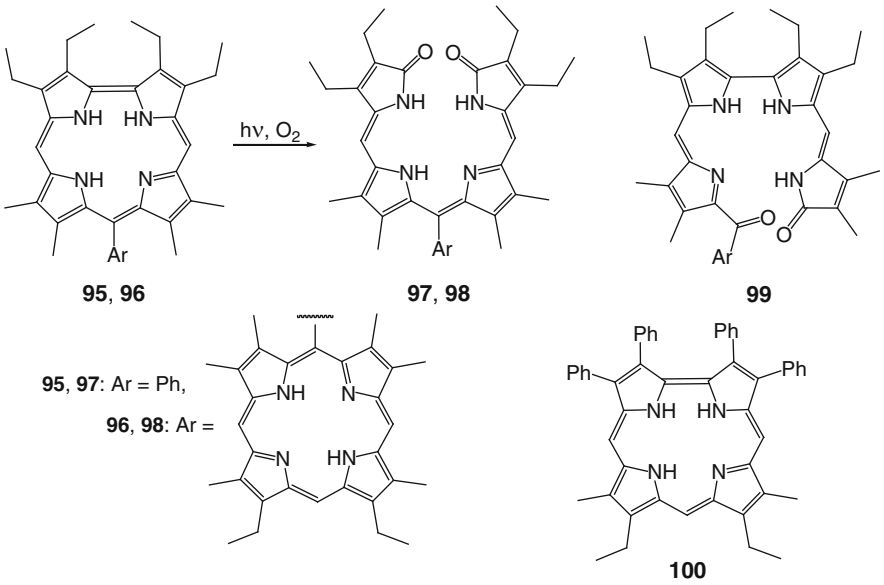

Scheme 29 Photooxidation of *meso*-aryl-substituted corroles **95**, **96** [143, 144]. An alternative structure of degradation product **99** and a tetraphenyl analogue of compound **95** are also shown

degradation product was made by Guilard and coworkers who investigated photooxidation of 2,3,17,18-tetraethyl-7,8,12,13-tetramethyl-10-phenylcorrole **95** (Scheme 29) [143]. A biliverdin derivative **97** was obtained in 24% yield and characterized by ^{1}H NMR, IR, MS and elemental analysis which were in general agreement with an intuitive assumption that pyrrole–pyrrole (C(1)–C(19)) bond was attacked by dioxygen molecule. No other reaction products were isolated. Opening of corrole ring by breaking of C(α)–C(α) bond was also postulated by Paolesse et al. for photooxidation of β-octaalkylcorrole with a porphyrin attached to a 10-position **96** [144]. In both cases the symmetry of resulting ^{1}H NMR spectrum was lower than expected for the proposed structure (an analogous triarylbilindione obtained by Yamauchi et al. by coupled oxidation of iron porphyrin exhibited a simple ^{1}H NMR pattern [145]). The difference was attributed to isomerization of biliverdin moiety to (*E*,*Z*,*Z*) configuration; however, certain spectral features (e.g. a doublet at ca. 8 ppm which could be assigned to *ortho*-aryl protons) suggest that a structure resulting from opening at aryl-substituted *meso* position **99** could be considered as well. On the other hand, the observation that 2,3,17,18-tetraphenyl analog **100** (*meso*-unsubstituted!) was found far more stable than **95** and a similar behavior of corresponding cofacial bis(corroles) connected with a 10-anthracene bridge suggested efficiency of a steric protection of bipyrrole fragment limiting the access of dioxygen molecule to C(1)–C(19) bond [146].

Degradation of *meso*-triarylcorroles has received a considerable attention [141, 142], but only a systematic mass spectrometry study on decomposition pathways of these compounds by Świder et al. led to identification of isocorroles and biliverdin

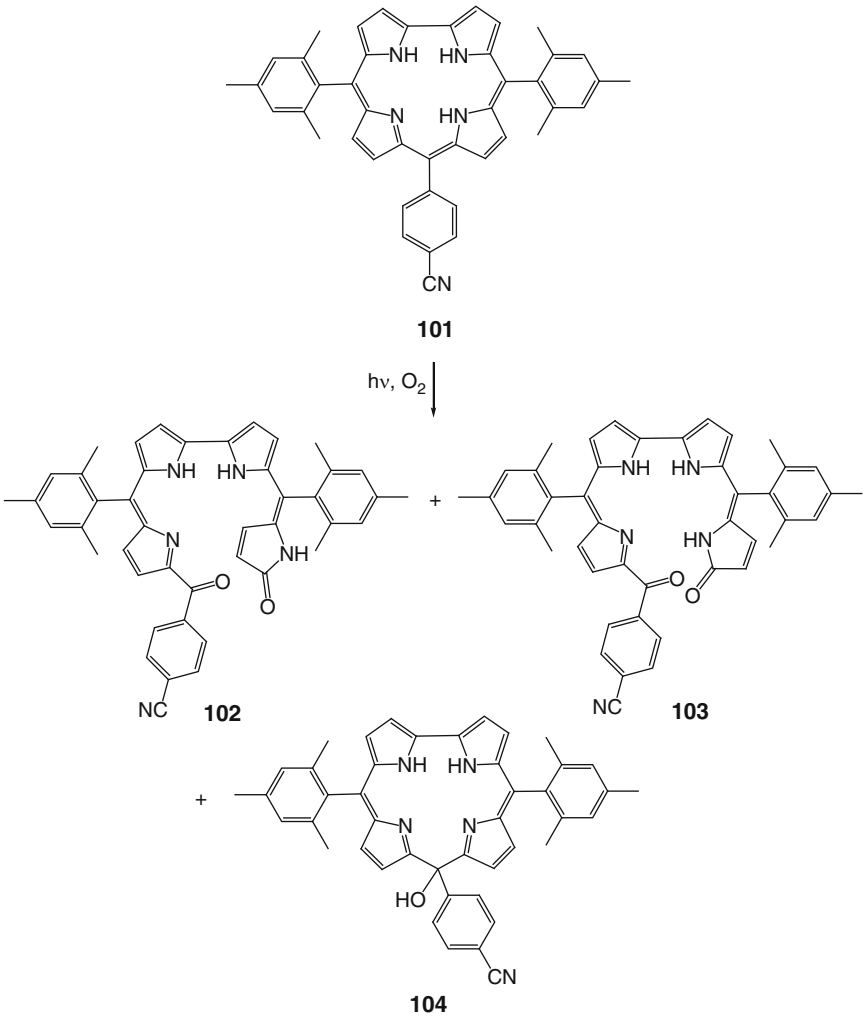

Scheme 30 Photooxidation of triarylcorrole [36]

derivatives as photooxidation products [36]. Preparative degradation experiment was conducted with corrole **101** with 5 and 15 positions protected by bulky substituents, which was dissolved in acetonitrile and exposed to sunlight for 60 h. Three major compounds **102**–**104** were isolated from the reaction mixture (Scheme 30), indicating dioxygen attack on *meso*-C(10) carbon atom. In our studies on photooxidation of triphenylcorrole and tris(*p*-methoxyphenyl)corrole, scission of C(9)–C(10), but also of C(4)–C(5) bond of symmetrical, non-hindered substrate was noted [147]. As can be seen, any product resulting from breaking of a direct pyrrole–pyrrole bond has not been detected from photodegradation of triarylcorroles. One couldn't exclude, however, that the presence of β-alkyl substituents in compounds **95**, **96** directs dioxygen

attack to the C(1)–C(19) bond. A strong dependence of reaction outcome on substitution of macrocycle is illustrated by reactivity of 5,10,15-tris(pentafluorophenyl) corrole which stirred at room temperature under ambient light and air slowly converted to 3,3′-linked dimer and 3,3′,17′,3″-trimer [148].

5 Coupled Oxidation

Heme oxygenase, responsible for the oxidative destruction of unwanted heme, requires molecular oxygen but also the source of electrons for its function (see Sect. 6 of this contribution). Oxidation of iron porphyrin in pyridine in the presence of reducing agent (hydrazine or ascorbic acid) has been used as a model for the enzymatic reaction [149, 150]. Pioneering studies by Lemberg (who described coupled oxidation of iron protoporphyrin IX with H_2O_2-ascorbic acid), Fischer and Libowitzky were performed on natural heme derivatives [151, 152]. Later on, higher symmetry synthetic model compounds such as complexes of octaethylporphyrin or ethioporphyrins have been used. A thorough analysis of coupled oxidation process was presented in a series of papers published in the years 1992–2008 by Balch, Latos-Grażyński, and coworkers. They isolated and characterized two main products of degradation of (OEP)$Fe^{II}(py)_2$ **105** caused by air in the presence of ascorbic acid: a diamagnetic verdoheme **106** (50%) and a paramagnetic dimeric iron biliverdin complex **107** (38%, Scheme 31) [153, 154]. In situ monitoring of the degradation of (OEP)$Fe^{II}(py)_2$ by dioxygen with hydrazine as sacrificial reductant identified iron oxophlorin, (OEPO)$Fe(py)_2$ **11** as a key intermediate of the process [155].

Oxidation of (OEP)$Fe^{III}Cl$ under pyridine-free conditions, but in the presence of cyanide ions as axial ligands, was also demonstrated [156]. Depending on cyanide concentration, iron oxophlorin or 5-oxaporphyrin complex (verdoheme) was formed. Coupled oxidation of Co(II) octaethylporphyrin leading to cobalt verdoheme and biliverdin analogs was also described [157]. In the recent years, degradation of iron complexes of β-unsubstituted, *meso*-arylporporphyrins under coupled oxidation conditions was investigated as well [145, 158–160].

5.1 Oxophlorins

The question of structure and reactivity of oxophlorins (hydroxyporphyrins) has been considered in numerous contributions. In addition to tautomeric equilibrium (Scheme 32), ocatethyloxophlorin was shown to undergo a facile one- and two-electron oxidation [161]. In consequence, it can serve as a trianionic, dianionic, and monoanionic ligand, and various electron distributions between metal ion and ligand are possible. Not surprisingly then, a rich coordination chemistry was observed for octaalkyloxophlorins: zinc(II), nickel(II), cobalt(II), copper(II), iron (III), and manganese(III) monomeric complexes with *meso*-hydroxyl groups

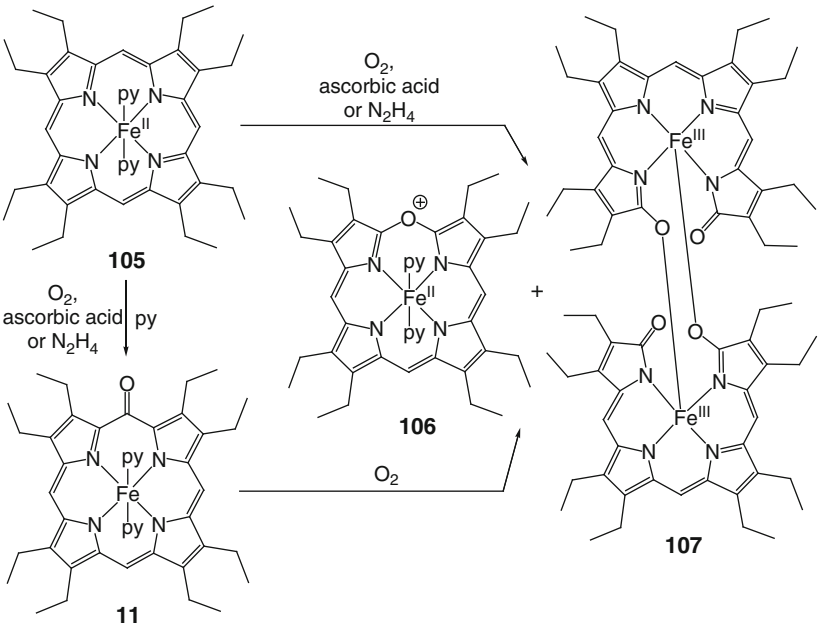

Scheme 31 Coupled oxidation of $(OEP)Fe^{II}(py)_2$ [153–155]

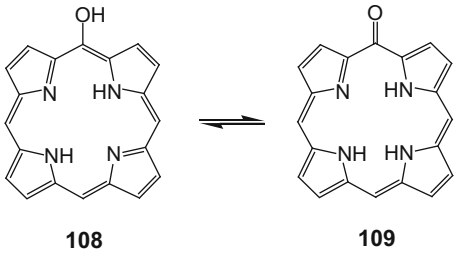

Scheme 32 Keto-enol tautomeric equilibrium of oxophlorin

[14, 162–166], dimeric complexes linked by *meso*-oxygen bridges with Fe(III), Mn(III), and In(III) [162, 165, 167–171], coordinated oxophlorin trianions [165, 166], coordinated radicals [163, 164, 168], and complexes of oxidized monoanionic form [168, 170] were reported. Variety of structures and their mutual interconversion is exemplified by iron(III) complexes shown in Scheme 33 [161]. The thorough overview of coordination chemistry of oxophlorins/*meso*-hydroxyporphyrins was published by Balch in 2000 [161].

Electronic structure of iron oxophlorin $(OEPO)Fe(py)_2$ and its analogs was a subject of a long-lasting debate [162, 167, 172–175]. Three possible electron distributions have been taken into account (Fig. 8). Patterns of paramagnetically shifted ^1H NMR signals observed for $(OEPO)Fe(py)_2$ and related species suggested a significant contribution of a ligand radical form $(OEPO^{\bullet})$–Fe^{II} [162, 172, 173]. A similar alteration of isotropic shifts was found for iron triphenyloxophlorin

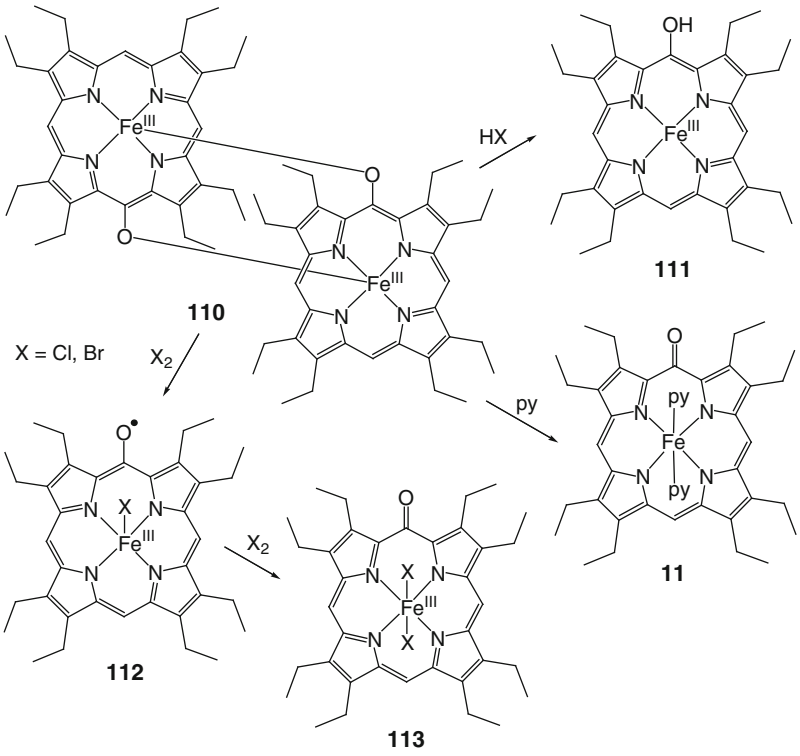

Scheme 33 Iron complexes of octaethyloxophlorin [161]

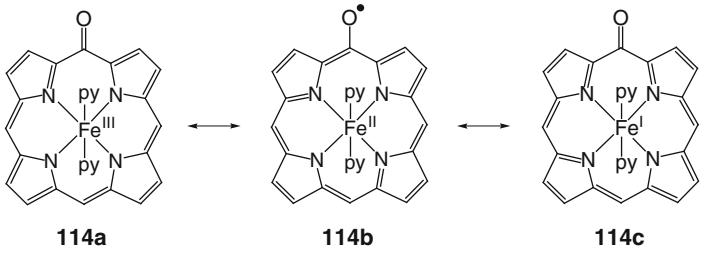

Fig. 8 Resonance forms of iron oxophlorin

complexes [158]. DFT calculated spin density maps for oxophlorin radicals allowed to reproduce the major observed spectroscopic features [176]. Later on, Rath et al. showed the dependence of electronic structure on the nature of axial ligands, with 2,6-xylyl isocyanide stabilizing the radical resonance structure $[(OEPO^{\bullet})Fe^{II}(CNR)_2]$ [177]. Recent crystallographic, magnetic, and spectroscopic measurements indicated the importance of Fe(III)/oxophlorin trianion form for bis-pyridine and bis-imidazole complexes [178]. DFT calculations of electronic structure of $(OEPO)FeL_2$ complexes

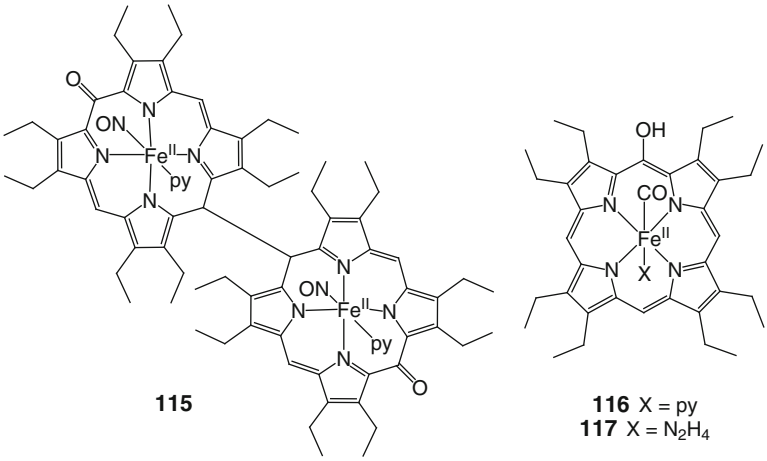

Fig. 9 Iron oxophlorin NO and CO complexes

performed by Gheidi et al. confirmed the dependence of electron distribution and iron spin state on the nature of axial ligands [179].

Reactivity of iron oxophlorin (OEPO)Fe(py)$_2$ (**11**) was extensively explored. Apart from coordination chemistry depicted in Scheme 33, interaction with small molecules was investigated [180, 181]. A reversible binding of NO to (OEPO)Fe(py)$_2$ connected with the formation of dimeric species **115** was reported (Fig. 9) [180]. A reduced form of oxophlorin, (OEPOH)Fe^{II}(py)$_2$, was converted to (OEPOH)Fe^{II}(CO)(py) (**116**) upon treatment with carbon monoxide, and pyridine could be replaced with hydrazine to form (OEPOH)Fe^{II}(CO)(N$_2$H$_4$) (**117**); both diamagnetic complexes were found extremely air sensitive and in the presence of dioxygen an immediate reaction leading to (OEPO)Fe(py)$_2$ **11** was observed [181].

Both redox processes preserving a basic skeleton of oxophlorin [168, 170] and coupled oxidation leading to verdoheme and biliverdin have been reported [155, 156]. Under certain conditions, oxidative degradation is not limited to macrocycle opening. Rath et al. observed that in the absence of reducing agent, addition of dioxygen to a pyridine solution of oxophlorin complex (OEPO)Fe(py)$_2$ (**11**) caused stepwise changes, resulting in formation of iron biliverdin **118**, and, finally, oxidative removal of pyrrole unit yielding a linear tripyrrole complex **38** (Scheme 34) [182]. This compound was also formed when compound **118** or verdoheme **106** was exposed to O$_2$.

5.2 Verdohemes

A green iron complex of 5-oxaporphyrin, called verdoheme, is an important intermediate in the process of heme oxidative cleavage by heme oxygenase [183]. It is also formed in the course of coupled oxidation of iron porphyrins but can be also obtained by dehydration of biliverdin in the presence or iron salts [184, 185].

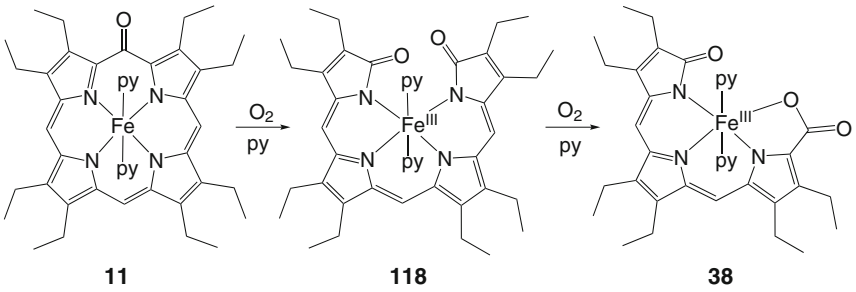

Scheme 34 Conversion of iron oxophlorin to a linear tripyrrole complex [182]

Metal-centered reactions have been reported, including changes of axial ligation, and metal oxidation and spin state, as demonstrated for iron (Scheme 35) and cobalt 5-oxaporphyrin complexes [153, 172, 186–192]. Coordination chemistry of verdohemes and biliverdin derivatives has been recently reviewed by Balch and Bowles [193].

Ligand transformations are particularly important for the study of macrocycle degradation since they can lead to linear tetrapyrrolic products. Two mechanisms of verdoheme ring opening leading to biliverdin have been described: an oxidative pathway [194, 195], resulting in release of Fe^{3+}, and a hydrolytic route (Scheme 36). The latter is generally believed to begin with addition of hydroxide to the macrocycle. To characterize this kind of reactivity of 5-oxapophyrin complexes, their conversions by anionic nucleophiles have been investigated [196–200]. Helical, ring-opened products resulting from the addition of alkoxide, thiolate, and amide ions to zinc(II) (**125**) and cobalt(II) verdoheme (**126**) were isolated and structurally characterized (Scheme 37) [197, 201]. More complex process was observed when cyanide ion was added to zinc 5-oxaporphyrin **125**, as macrocycle cleavage was accompanied with substitution at one or two *meso* positions (Scheme 38) [199]. A dimeric complex $[(OEBOMe)Fe^{II}]_2$ **130** was isolated from the reaction of iron(II) verdoheme with OMe^- ion (Scheme 39) [198]. Ring opening of Fe^{II} and Fe^{III} verdohemes with methoxide or hydroxide was monitored by ^1H NMR spectroscopy [200]. Characteristic alternating shift patterns indicating radical character of the particular intermediates and remarkable paramagnetic shifts of *meso* resonances of certain species were noted.

Utilizing O_2 as oxidant, Rath et al. demonstrated a conversion of Fe(II) verdoheme into a highly oxidized (Fe(IV) bound to bilindione ligand or Fe(III) coordinated to oxidized form of ligand) biliverdin complex (Scheme 40) [195]. Its reduction with zinc amalgam resulted in previously characterized dimeric $[(OEB)Fe^{III}]_2$ (**107**). Earlier, Saito and Itano reported that prolonged (1 month) exposure to air of verdoheme dissolved in ethylene glycol – pyridine solution led to several iron-free ring-opened products, including tripyrrolic ones [202]. Most of the starting material was recovered from the reaction.

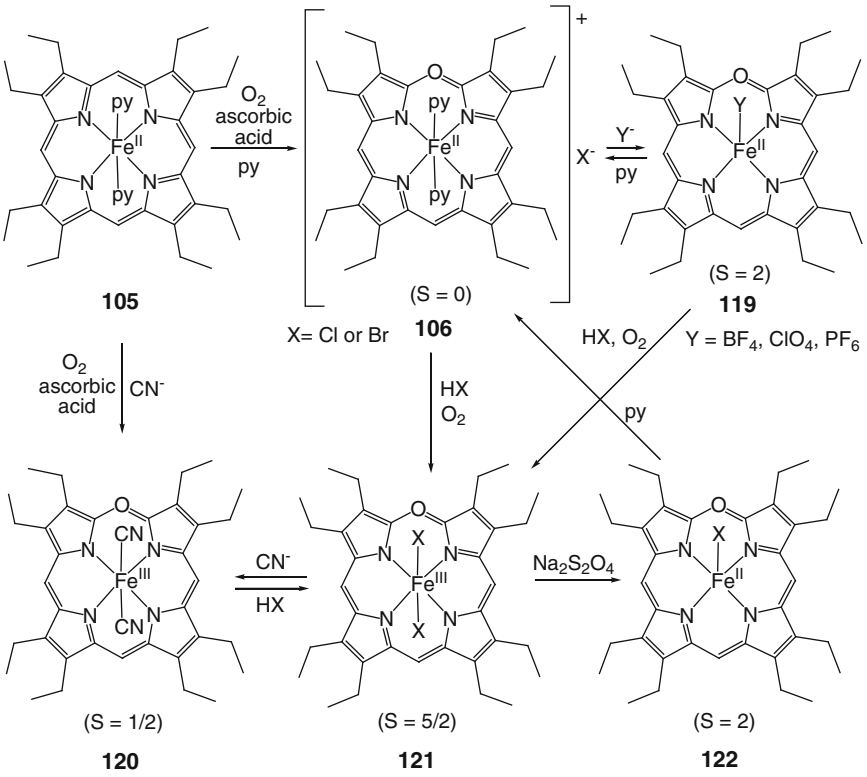

Scheme 35 Interconversion of iron 5-oxaporphyrin complexes [193]

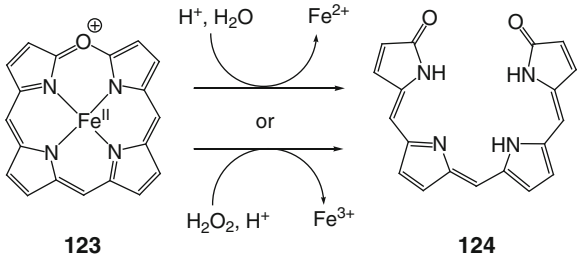

Scheme 36 Two pathways of verdoheme to biliverdin coversion

Theoretical study on factors determining verdoheme conversion to biliverdin was performed by Safari and coworkers. The role of axial ligands as well as coordinated metal ion was taken into account [203–206].

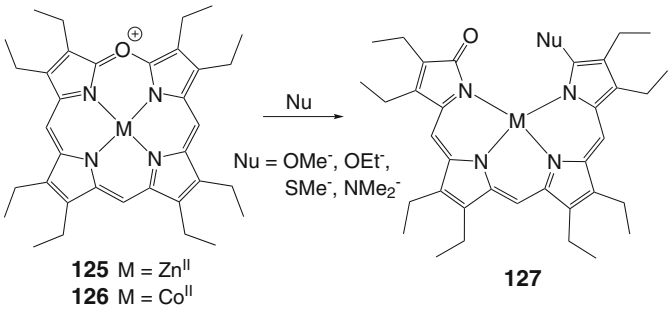

Scheme 37 Opening of zinc(II) and cobalt(II) verdohemes by nucleophiles [197, 201]

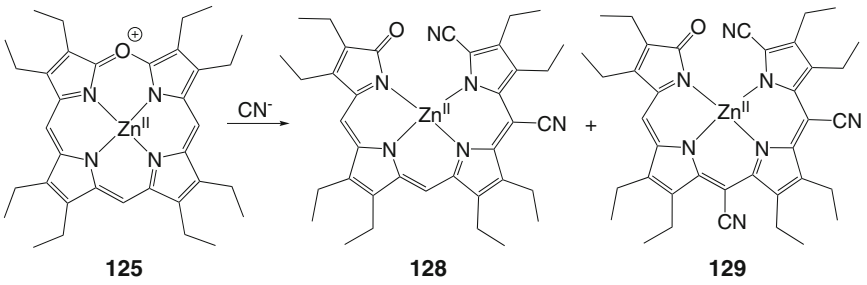

Scheme 38 Zinc(II) verdoheme opening by cyanide [199]

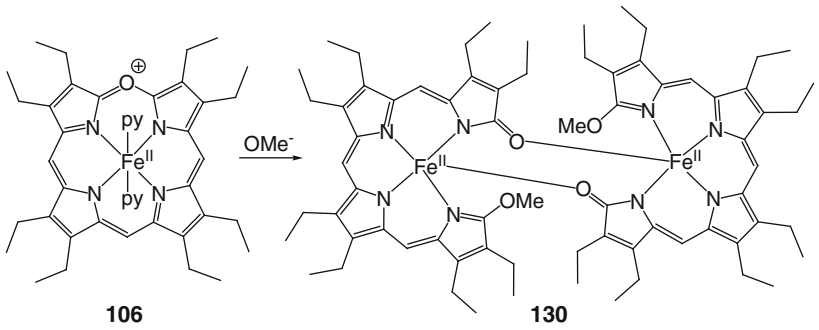

Scheme 39 Reaction of iron(II) verdoheme with methoxide [198]

5.3 Biliverdins

A dimeric helical iron(III) complex **107** of octaethylbilindione, a biliverdin analog, was obtained by Balch et al. along with verdoheme from the coupled oxidation of $(OEP)Fe^{II}(py)_2$ [154]. Its treatment with pyridine resulted in cleavage of Fe–O bonds and formation of monomeric $(OEB)Fe^{III}(py)_2$ **132** (Scheme 41). An easy

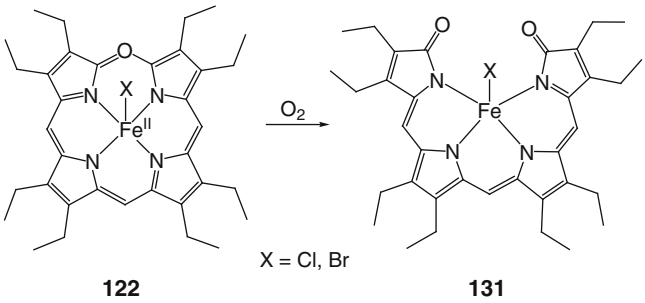

Scheme 40 Oxidation of iron(II) verdoheme [195]

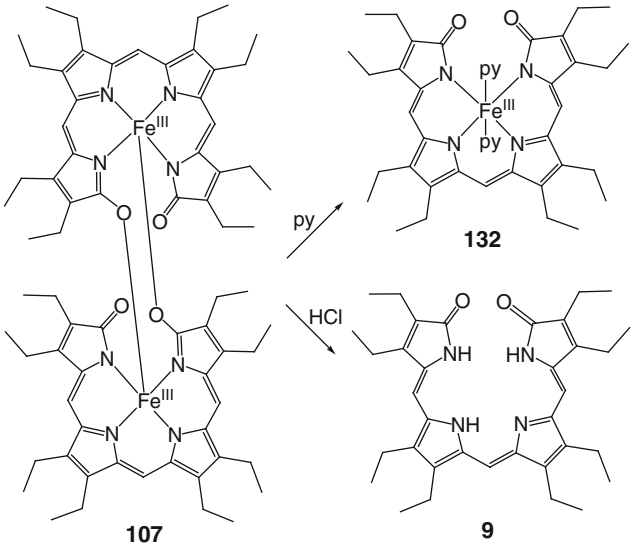

Scheme 41 Splitting of dimeric iron(III) octaethylbiliverdin complex [154]

demetallation of $[(OEB)Fe^{III}]_2$ with hydrochloric acid released the blue bilindione $OEBH_3$ (**9**) [154]. Its complexes with other metal ions were investigated by Bonnett and coworkers [207, 208] and by Balch group [13, 209–215]. Interestingly, remetallation of $OEBH_3$ with iron has not been successful [193], while manganese, cobalt, nickel, copper, zinc, palladium, and boron complexes have been obtained. For Mn(III), a dimeric complex with oxygen bridges $[(OEB)Mn^{III}]_2$, which was cleft by pyridine to monomeric $(OEB)Mn^{III}(py)_2$ (in a full analogy with Fe(III) complexes) was described [210]. Spectroscopic investigations of monomeric, four-coordinate complexes of $OEBH_3$ with cobalt, nickel, copper, and palladium suggested their electronic structure consistent with the presence of M(II) ion and oxidized ligand radical $(OEB^{\bullet})M^{II}$ [208–210, 214] A significant degree of radical character was also postulated for iron complexes obtained by verdoheme ring

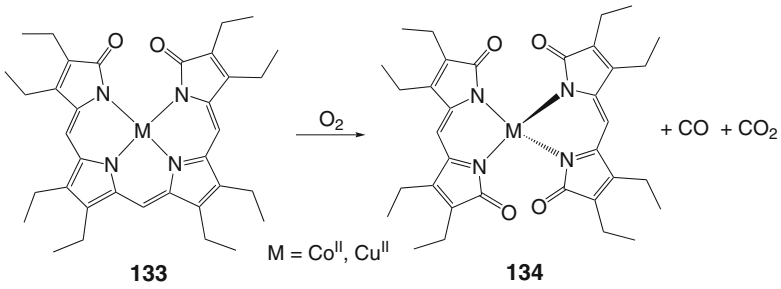

Scheme 42 Oxidation of cobalt and copper biliverdin complexes [209, 213]

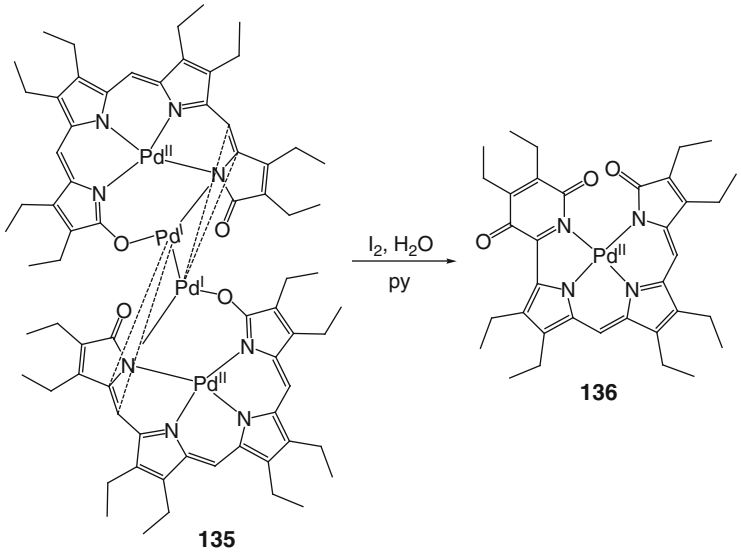

Scheme 43 Oxidation of tetranuclear palladium biliverdin complex by I_2 [215]

opening [200]. Cobalt biliverdins were alternatively obtained by a coupled oxidation of Co(II) octaethylporphyrin [157]. Oxidation with iodine converted (OEB$^{\bullet}$) M^{II} complexes (M = Co, Ni, Pd) into ones containing an oxidized form of bilindione ligand [211, 214], while aerial oxidation of copper and cobalt complexes **133** resulted in cleavage of tetrapyrroles yielding complexes with two coordinated dipyrrolic units **134** (Scheme 42) [209, 213].

A unprecedented tetranuclear complex **135** consisting of two helical (OEB)Pd^{II} units bridged by $(Pd_2^{I})^{2+}$ fragment was isolated along with monomeric (OEB)Pd from the insertion of palladium into OEB ligand [13, 214, 215]. Reaction of this compound with iodine resulted in formation of rearranged monomeric complex **136**: an incorporation of oxidized *meso*-carbon into a terminal pyrrolone unit was observed (Scheme 43)[215].

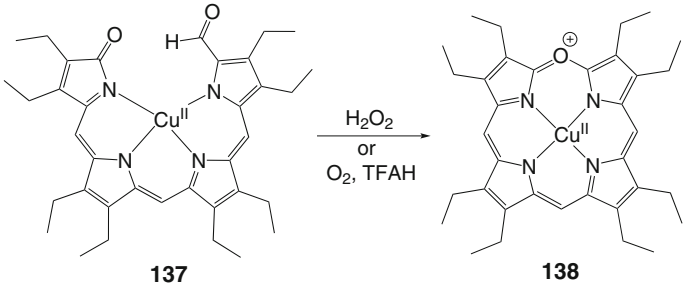

137 **138**

Scheme 44 Conversion of copper(II) formylbiliverdin to verdoheme [9]

Oxidative cyclization of biliverdin complexes leading to metalloverdohemes was also studied [216]. Nickel(II), cobalt(II), and copper(II) octaethylformylbiliverdins were converted to verdoheme analogues by treatment with hydrogen peroxide or (in case of Cu(II) species) by heating with trifuoroacetic acid under dioxygen (Scheme 44) [9]. Formation of carbon monooxide and dioxide was detected in the course of the reaction. Addition of trifluoroacetic acid to the dichloromethane solution of palladium octaethylbilindione also resulted in ring closure. Only 5 min of stirring at room temperature was found sufficient to cause the transformation [215] .

Formation of biliverdin derivatives in a process of coupled oxidation of iron porphyrins is not limited to β-octaalkyl derivatives. Mizutani's group worked out a high-yielding method of preparation of tetraphenylbiladienone **20** (a major product of degradation of TPP complexes by Tl(III), Ce(IV) or photooxidation, see Sects. 3.1 and 4.1) [145, 159, 160]. Iron *meso*-tetraphenylporphyrin subjected to coupled oxidation procedure in a chloroform solution yielded a mixture of isomeric biladienones **20** (63%) and **140** (15%; Scheme 45) [145]. Compound **140** could be photoisomerized to **20**, while the reverse transformation did not proceed. The additional bilindione products **141**, **142** were obtained when the reaction was carried out in refluxing chloroform; both compounds were converted to each other with visible light illumination. An X-ray structure of isomer **141** proved its *ZZZ* configuration and a helicoidal conformation. The procedure could be extended to other tetraarylporphyrins substituted in *para* positions with OCH_3, $COOCH_3$, CN, $OC_{12}H_{25}$, and $COOC_{12}H_{25}$ groups [159, 160]. The reaction was accelerated by electron-withdrawing substituents, which also favored the formation of triarylbilindiones (maximum yield of 19% was noted for *p*-$COOC_{12}H_{25}$ derivative) while electron-donating ones increased the amounts of biladienones (85% yield for methoxy-substituted substrate was found). Interestingly, the presence of one methoxy substituent in *ortho* position of each of phenyl groups did not prevent the macrocycle from oxidative degradation: both biladienone and bilindione were formed in 14% and 10% yield, respectively. Cyclization of bilindiones **141** was also described yielding the corresponding zinc triarylverdohemes, which were isolated as trfiluoroacetates [217].

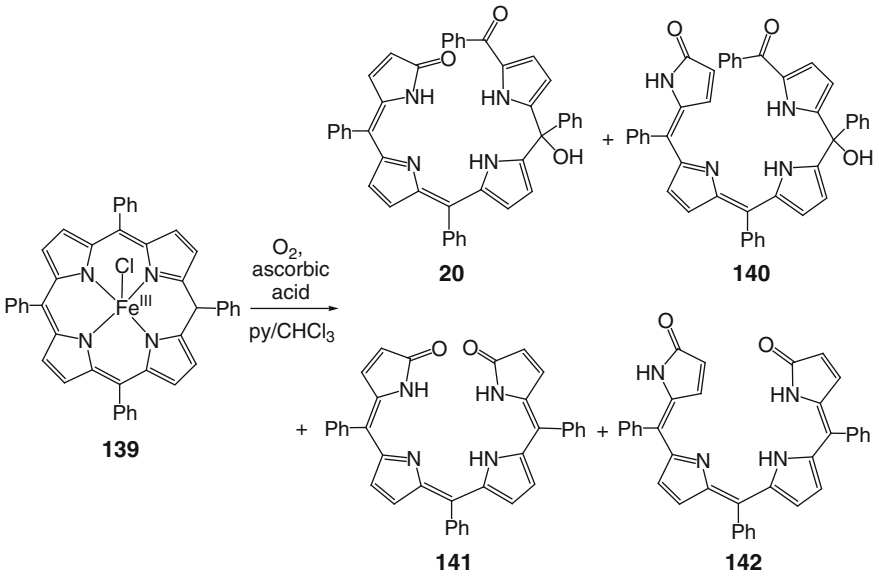

Scheme 45 Coupled oxidation of iron(III) tetraphenylporphyrin [145]

Theoretical studies on biliverdin and its complexes involved such aspects as molecular and electronic structure of its isomeric forms [218] and biliverdin-based metalloradicals [219], spin density distribution in metallobiliverdin radicals [220], energetics and dynamics of dimer formation by oxidized species [221], and mechanism of reduction to bilirubin [222].

5.4 Regioselectivity of Coupled Oxidation

Studies on regioselectivity of coupled oxidation of iron porphyrins were aimed to establish the influence of factors connected with a structure of macrocyclic substrate on the outcome of degradation process. Four isomeric biliverdins were isolated in comparable yields from coupled oxidation of iron(III) protoporphyrin IX, thus regioselectivity observed in natural systems (see Sect. 6) was lost [223, 224]. Later studies showed that replacement of 3-methyl group of mesoheme with CF_3 substituent had a great influence on product distribution: ring-opening occurred mainly at C(20) yielding δ isomer as a major product [225].

Coupled oxidation of 5- or 15-phenyl-substituted iron(III) protoporphyrin IX in pyridine solution yielded biliverdins opened only at three unsubstituted *meso* positions (as illustrated in Scheme 46 for 5-phenyl derivative) [35, 226]. Similarly, 5-aryl-mesohemes III were cleft at C(10), C(15) or C(20) yielding (due to symmetry of the starting complex) only two isomeric products [227]. The character of

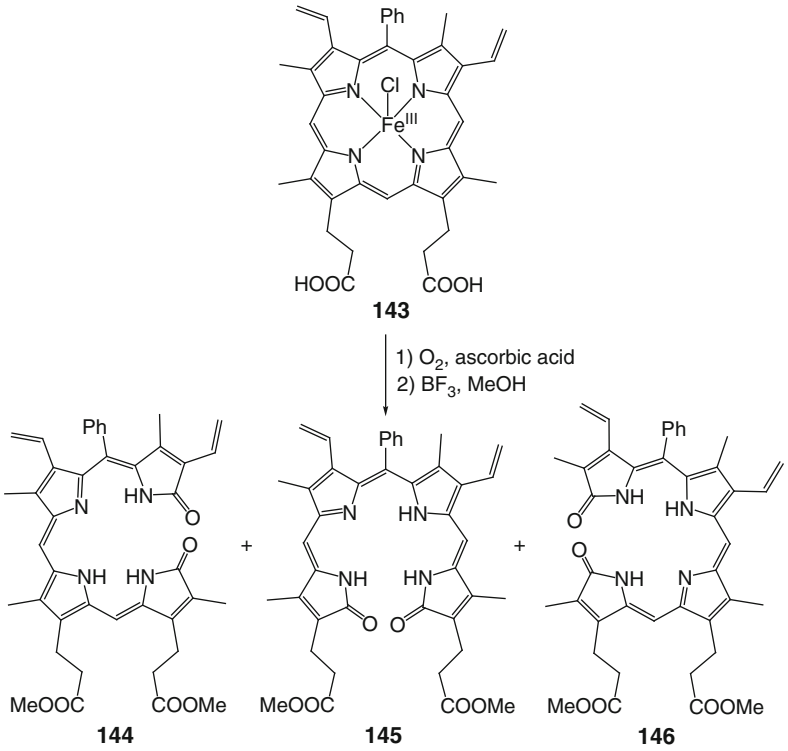

Scheme 46 Coupled oxidation of 5-phenylprotoheme [35]

aryl ring substituent influenced the reaction yield, but its impact on the product distribution was rather negligible. The identified biliverdin isomers served as references for studies on the regioselectivity of heme oxygenase (see Sect. 6 of this contribution) [228].

6 Biodegradation of Tetrapyrrolic Macrocycles

Degradation of tetrapyrrolic macrocycles is used by living organisms both as a method of removal of unwanted (redundant) heme or chlorophyll and as a way of synthesis of linear systems (bilins) which can also fulfill important physiological functions [229–232]. Mechanism of transformation of macrocycles to acyclic oligopyrroles has now become much more clear and better understood in the result of numerous studies on model reactions and determination of active intermediates and structures of key enzymes.

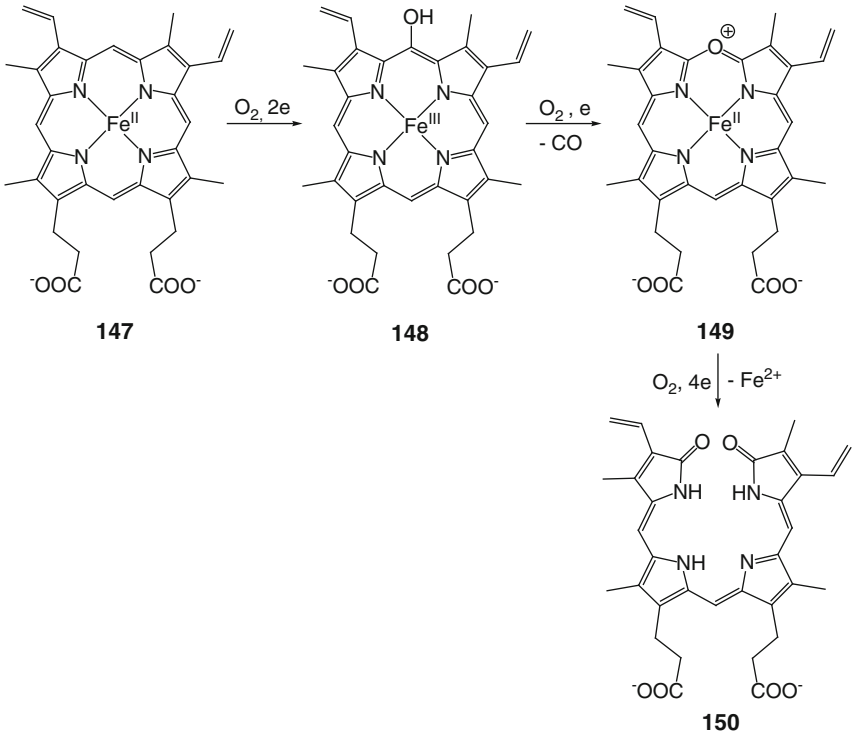

Scheme 47 Heme degradation catalyzed by heme oxygenase

6.1 Heme Oxygenase

Heme oxygenase (HO), an enzyme responsible for the oxidative conversion of heme to biliverdin, was discovered by Tenhunen et al. in 1968 [233]. Since that report, numerous studies have been devoted to understanding the mechanism of the enzymatic action [183, 234–239]. HO is unique among heme enzymes in that activation of dioxygen by prosthetic group is utilized for its own degradation. A regiospecific conversion of heme to biliverdin IXα, carbon monooxide and Fe^{2+} ions requires three molecules of O_2 and the total uptake of seven electrons, and proceeds in three successive steps (Scheme 47): *meso*-hydroxylation, followed by release of CO and verdoheme formation and ring opening connected with iron loss yielding free biliverdin. Formation of such metabolites implies other functions of heme oxygenase, involving iron homeostasis, cytoprotection against oxidative injury and cellular stress, and postulated role in cellular signaling.

In mammals three isoforms of HO have been identified; heme degradation enzymes can also be found in plants and some pathogenic bacteria [183, 240–242]. Many of these proteins have been structurally characterized, including cofactor-free enzymes and their complexes with heme and subsequent intermediates of its enzymatic conversion [240, 241, 243–248]. Since the structural aspects and mechanism of heme

oxygenase have been thoroughly reviewed [183], only chosen aspects of recent investigations in the field will be presented in this contribution.

Several groups concentrated their efforts on detailed analysis of mechanism of heme degradation. A theoretical study on *meso*-hydroxylation step by Shaik and coworkers indicated a preference for homolytic dissociation of O–O bond in Fe–OOH intermediate and the crucial role of hydrogen bonding network of distal heme pocket in trapping of $^{\bullet}$OH radical, in full agreement with the experimental data [249–251]. Verdoheme opening, the less understood third step of degradation process, was investigated by Ikeda-Saito and coworkers [239]. They prepared verdoheme complexes with various heme oxygenases and characterized them by various techniques [245, 252, 253]. A similarity of the final stage of heme oxidation to the first one was observed, including the participation of water cluster in the radical intermediate binding. Verdoheme-heme oxygenase complexes were also characterized by other groups [246, 254, 255].

Factors influencing regioselectivity of heme degradation have been also studied. The exclusive formation of α isomer of *meso*-hydroxyheme and, finally, of biliverdin α was substantiated by specific seating of heme in the protein and the construction of distal pocket limiting the access of coordinated dioxygen molecule to other *meso* positions [183, 236]. Mutant heme oxygenases were prepared with an altered regioselectivity which was attributed to various possible orientations of heme moiety [256, 257]; mutations can even change the typical function of enzyme to peroxidase activity [258]. Bacterial heme oxygenases were characterized exhibiting different preference of heme oxidation site as a result of specific seating of the heme [241, 259–261]. Part of regioselectivity studies utilized modified hemes to explore the impact of porphyrin ring substitution on the degradation process. Heme oxygenase was shown to accept various iron porphyrins as substrates, though the presence of propionate chains at C(13) and C(17) seemed to be an important feature required for enzymatic action [183, 234, 262]. Ikeda-Saito and coworkers showed that HO is capable of oxidizing of all isomers of *meso*-hydroxyhemin to the corresponding verdohemes, but only verdoheme α was further converted to biliverdin [263]. *Meso*-substitution effects were particularly important for the analysis of ring-opening mechanisms. Oxidation of mesoheme with methylated *meso*-position by human HO-1 was investigated by Torpey and Ortiz de Montellano [264]. Surprisingly, α-CH_3-derivative was converted to biliverdin α, while γ-CH_3-mesoheme yielded exclusively γ isomer (Scheme 48; in both cases the fate of extruded *meso* substituent remained unknown); β and δ-substitution resulted in a mixture of products (both methylated and *meso*-unsubstituted).

When protoheme substituted with 5- or 15-phenyl group was used as a substrate, biliverdin α was formed (Scheme 49; benzoic acid by-product was isolated in the first case) [228]. Mesobiliverdin α was identified as the major degradation product of various 5-aryl-mesohemes; isoporphyrin intermediate was detected in this reaction [265]. In contrast, 5-formylmesohemes were exclusively oxidized by heme oxygenase at non-substituted carbons (C(10) or C(20)) to give a formylated biliverdin derivative [266]. Generally, product distribution was found dependent mainly on the possible orientations of modified heme in the protein crevice, but electronic effects of substituents were also of importance.

Scheme 48 Oxidation of methylated mesoheme by human HO-1 [264]

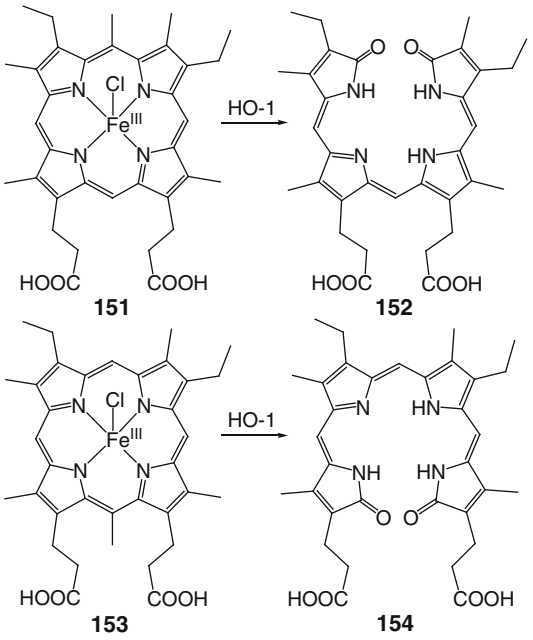

Scheme 49 Oxidation of phenyl-substituted protoheme by HO-1 [228]

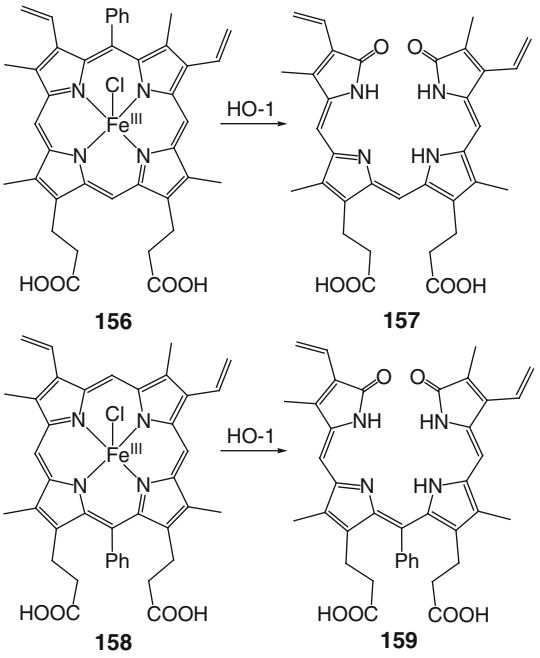

The observation that under certain conditions various heme proteins also can exhibit oxygenase activity led to elaboration of protocol of coupled oxidation, which was used as a model of enzymatic heme degradation [267]. Though the detailed mechanism of *meso*-hydroxylation step is slightly different [237, 268], both processes share common intermediates: hydroxyheme, verdoheme, and, finally, iron- and metal-free biliverdin. In a typical experiment, these compounds are produced upon treatment of heme protein with an excess of ascorbate and dioxygen or H_2O_2; sometimes also the addition of pyridine was necessary to replace the protein axial ligands [231]. Coupled oxidation of hemoglobin (Hb) and myoglobin (Mb) has been most widely studied, leading mainly to α isomer of biliverdin, but in case of Hb a significant amount of β isomer is also produced [194, 269, 270]. This regioselectivity is changed for abnormal or mutant hemoglobins [270, 271] as well as for cobalt(II) porphyrins used as substrates [272]. Coupled oxidation of heme covalently attached to a variant of *Escherichia coli* cytochrome b_{562} yielded a verdoheme protein complex which could be converted with formic acid to protein-attached α-biliverdin [273]. One of axial ligand mutants of mitochondrial cytochrome b_5, H63V, also stopped at the verdoheme stage while H39V variant allowed to oxidize heme to biliverdin [274]. This different behavior was attributed to the presence of polar amino acid residues in H39V mutant able to interact with heme-bound iron.

6.2 Chlorophyll Degradation

The principal transformations and main intermediates of chlorophyll breakdown have been identified [275–278]. Chlorophyll *a* **160** and chlorophyll *b* **161** lose phytol side chain and magnesium ion and pheophorbide *a* **162** is formed (Scheme 50). Ring opening occurring exclusively at C(5) *meso* position yields a tetrapyrrole called red chlorophyll catabolite (RCC, **163**) which is further converted to fluorescent and nonfluorescent chlorophyll catabolites (FCCs and NCCs, respectively). A key ring-opening step is catalyzed by a specific enzyme, pheophorbide a oxygenase [279, 280]. Isotope labeling experiments showed that only one of newly introduced oxygen atoms is derived from O_2 molecule, while the second one probably originates from water.

Studies on photooxygenation of chlorophyll and bacteriochlorophyll derivatives were conducted in context of the catabolism of these compounds occurring in vivo. Typically, ring-opening reactions occurred by dioxygen attack on C(1)–C(20) bond [114, 281]. However, Iturraspe and Gossauer demonstrated the regioselectivity change by metal coordination: zinc(II) pyropheophorbide *a* methyl ester **16** led to C(20)-opened product **165** while cadmium complex **164** underwent cleavage of C(4)–C(5) bond yielding compound **166** (Scheme 51) [282]. Recent studies on the degradation of zinc chlorophyll derivatives substituted at 3- and 13-positions showed a systematic change of electronic absorption maxima (up to 919 nm) of the ring-opened products with the electron-withdrawing character of the substituent, demonstrating their attractiveness as near-infrared light absorbing pigments [283].

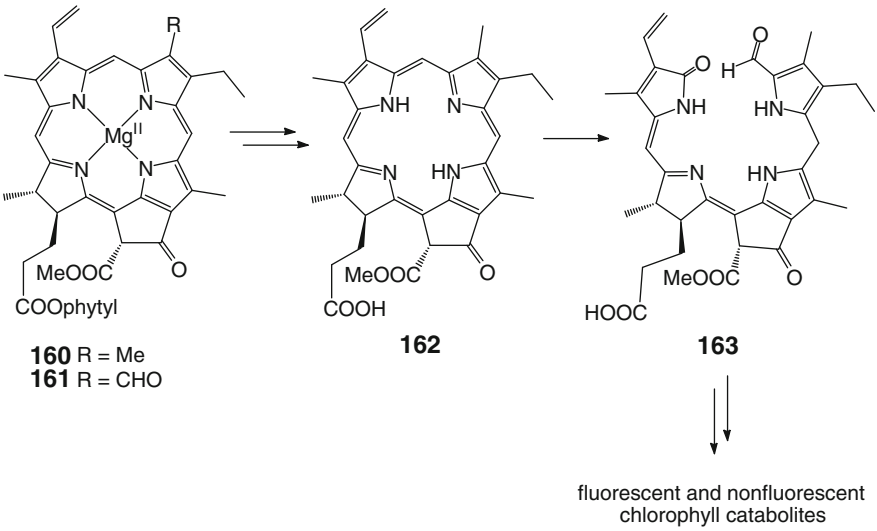

Scheme 50 Chlorophyll degradation

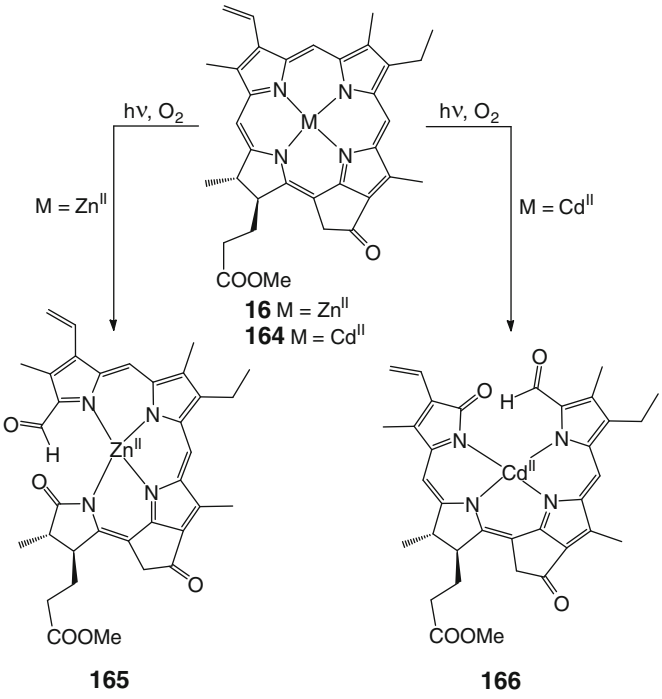

Scheme 51 Photooxidation of pyropheophorbide *a* derivatives [282]

7 Summary: Future Directions

The word "degradation" is commonly associated with the loss of quality, with a conversion of an object or a person to less attractive and less valuable state or form. These negative connotations, however, should not come to mind when porphyrin degradation is considered. Certainly, formed products lack many of properties of a parent compound, but at the same time they gained certain unique features, such as a conformational flexibility or an interesting coordination behavior. Ring opening of cyclic tetrapyrroles can be applied as the easiest method of preparation of these linear oligopyrroles.

On the other hand, many of degradation processes are not selective and are frequently accompanied by subsequent reactions (demetallation, *Z-E* isomerization, water/alcohol addition) which further increase the number of possible products. In many classical papers on porphyrin degradation, only major products were isolated and characterized, and the fate of the rest of starting material remains unknown. Perhaps the use of modern analytical techniques could lead to identification of minor decomposition products.

In general, a great progress has been made in deciphering of degradation processes of tetrapyrrolic macrocycles in nature and of their synthetic models. Still, some fields remain underexplored, including pathways of inactivation of metalloporphyrin catalysts. Since the ways of porphyrin ring modification are unlimited, new developments in the field can be expected because a specific reactivity can be generated connected with the particular substitution or/and metal ion insertion.

One can also imagine that wider synthetic availability of such members of porphyrinoid family, as expanded porphyrins, contracted ones, porphyrin isomers (N-confused, fused, porphycenes,...), and heteroporphyrins could result in investigations on their oxidative degradation. Ring opening of octaphyrins upon metallation with Cu(II) and interesting oxidative conversions of dithiaethyneporphyrin and dioxaporphyrin which were described quite recently show a potential hidden in these porphyrin analogs [284–286].

References

1. Adams KR, Bonnett R, Burke PJ, Salgado A, Vallés MA (1993) The 2,3-secochlorin-2, 3-dione system. J Chem Soc Chem Commun 1860–1861
2. Brückner C, Rettig SJ, Dolphin D (1998) Formation of a *meso*-tetraphenylsecochlorin and a homoporphyrin with a twist. J Org Chem 63:2094–2098
3. Sessler JL, Shevchuk SV, Callaway W, Lynch V (2001) A one-step synthesis of a free base secochlorin from a 2,3-dimethoxy porphyrin. Chem Commun 968–969
4. Pacholska E, Latos-Grażyński L, Ciunik Z (2002) A direct link between annulene and porphyrin chemistry − 21-vacataporphyrin. Chem Eur J 8:5403–5406

5. Pacholska-Dudziak E, Szterenberg L, Latos-Grażyński L (2011) A flexible porphyrin–annulene hybrid: a nonporphyrin conformation for *meso*-tetraaryldivacataporphyrin. Chem Eur J 17:3500–3511
6. Mizutani T, Yagi S, Honmaru A, Murakami S, Furusyo M, Takagishi T, Ogoshi H (1998) Helical chirality induction in zinc bilindiones by amino acid esters and amines. J Org Chem 63:8769–8784
7. Mizutani T, Sakai N, Yagi S, Takagishi T, Kitagawa S, Ogoshi H (2000) Allosteric chirality amplification in zinc bilinone dimer. J Am Chem Soc 122:748–749
8. Hamakubo K, Yagi S, Nakazumi H, Mizutani T, Kitagawa S (2006) Homohelicity induction of propylene-linked zinc bilinone dimers by complexation with chiral amine and α-amino esters. Preorganization of structurally coupled homohelical subunits. Tetrahedron 62:3619–3628
9. Koerner R, Olmstead MM, Ozarowski A, Phillips S, Van Calcar PM, Winkler K, Balch AL (1998) Possible intermediates in biological metalloporphyrin oxidative degradation. Nickel, copper and cobalt complexes of octaethylformybiliverdin and their conversion to a verdoheme. J Am Chem Soc 120:1274–1284
10. Mizutani T, Yagi S (2004) Linear tetrapyrroles as functional pigments in chemistry and biology. J Porphyr Phthalocyanines 8:226–237
11. Bröring M (2010) Beyond dipyrrins: coordination interactions and templated macrocyclizations of open-chain oligopyrroles. In: Kadish KM, Smith KM, Guilard R (eds) Handbook of porphyrin science with applications to chemistry, physics, materials science, engineering biology and medicine, vol 8. World Scientific, Singapore, pp 343–501 (Chapter 41)
12. Koerner R, Olmstead MM, Ozarowski A, Balch AL (1999) A linear tetrapyrrole as a binucleating ligand with copper(II). Coordination beyond the usual M–N_4 bonding. Inorg Chem 38:3262–3263
13. Lord P, Olmstead MM, Balch AL (1999) Tetrapyrroles as π donors: a Pd_2^{2+} unit sandwiched between two helical bilindione–palladium moieties. Angew Chem Int Ed 38:2761–2763
14. Phillips S, Noll BC, Olmstead MM, Balch AL (2001) Oxidation of copper(II) hydroxyporphyrin (oxophlorin); oxidative ring opening and formation of an ester-linked dinuclear copper complex. Can J Chem 79:922–929
15. Fuhrhop J-H (1975) Irreversible reactions at the porphyrin periphery (excluding photochemistry). In: Smith KM (ed) Porphyrins and metalloporphyrins. Elsevier, Amsterdam, pp 625–666 (Chapter 15)
16. Nicolaus RA, Mangoni L, Caglioti L (1956) Pyrrole acids in the oxidation of the porphyrins. Ann Chim (Rome) 46:793–805
17. Gray CH, Nicholson DC, Nicolaus RA (1958) The IX-alpha structure of the common bile pigments. Nature 181:183–185
18. Battersby AR, Cardwell KS, Leeper FJ (1986) Stereochemical studies on porphyrin a: assignment of the absolute configuration of a model porphyrin by degradation. J Chem Soc Perkin Trans 1 1565–1580
19. Chapman RA, Roomi MW, Morton TC, Krajcarski DT, MacDonald SF (1971) The analytical reduction of porphyrins to pyrroles. Can J Chem 49:3544–3564
20. Ficken GE, Johns RB, Linstead RP (1956) Chlorophyll and related compounds. Part IV. The position of the extra hydrogens in chlorophyll. The oxidation of pyrophœophorbide-*a*. J Chem Soc 2272–2280
21. Morley HV, Holt AS (1961) Studies on chlorobium chlorophylls. II. The resolution of oxidation products of chlorobium pheophorbide (660) by gas–liquid partition chromatography. Can J Chem 39:755–760
22. Purdie JW, Holt AS (1965) Structures of chlorobium chlorophylls (650). Can J Chem 43:3347–3353

23. Ellsworth RK, Aronoff S (1968) Investigations on the biogenesis of chlorophyll *a*. I. Purification and mass spectra of maleimides from the oxidation of chlorophyll and related compounds. Arch Biochem Biophys 124:358–364
24. Rüdiger W (1969) Chromsäure- und Chromatabbau von Gallenfarbstoffen. Z Physiol Chem 350:1291–1300
25. Bonnett R, McDonagh AF (1969) Methylvinylmaleimide (nitrite body) from chromic acid oxidation of tetrapyrrolic pigments. Chem Ind 107–108
26. Ellsworth RK (1970) Gas chromatographic determination of some maleimides produced by the oxidation of heme and chlorophyll *a*. J Chromatogr A 50:131–134
27. Martin J, Quirke E, Shaw GJ, Soper PD, Maxwell JR (1980) Petroporphyrins—II. The presence of porphyrins with extended alkyl substituents. Tetrahedron 36:3261–3267
28. Gauler R, Hesse U, Risch N (1995) Derivatives of natural tetrapyrroles for photodynamic therapy, 3. Oxidative degradation studies on porphyrins with chromic acid. Liebigs Ann 2227–2230
29. Risch N, Hesse U, Josephs A, Gauler R (1996) Derivatives of natural tetrapyrroles for photodynamic therapy, 4. Oxidative degradation studies: direct analysis and determination of ether and ester linkages in porphyrin dimers and oligomers of hematoporphyrin derivative (HPD). Liebigs Ann 1871–1874
30. Satoh Y, Nomoto S, Hama T (2012) Comprehensive determination of chlorophyll derivatives by chromic acid oxidation. Chem Lett 41:571–573
31. Byrn MP, Curtis CJ, Hsiou Y, Khan SI, Sawin PA, Tendick SK, Terzis A, Strouse CE (1993) Porphyrin sponges: conservation of host structure in over 200 porphyrin-based lattice clathrates. J Am Chem Soc 115:9480–9497
32. Hayes JM, Freeman KH, Popp BN, Hoham CH (1990) Compound-specific isotopic analyses: a novel tool for reconstruction of ancient biogeochemical processes. Org Geochem 16:1115–1128
33. Yu Z, Sheng G, Fu J, Peng P (2000) Determination of porphyrin carbon isotopic composition using gas chromatography–isotope ratio monitoring mass spectrometry. J Chromatogr A 903:183–191
34. Van Berkel GJ, Glish GL, McLuckey SA, Tuinman AA (1989) Mechanism of porphyrin reduction and decomposition in a high-pressure chemical ionization plasma. J Am Chem Soc 111:6027–6035
35. Niemevz F, Buldain GY (2004) Phenyl biliverdin isomers obtained by chemical oxidation of iron(III) complex of 5-phenyl protoporphyrin IX. J Porphyr Phthalocyanines 8:989–995
36. Świder P, Nowak-Król A, Voloshchuk R, Lewtak JP, Gryko DT, Danikiewicz W (2010) Mass spectrometry studies on *meso*-substituted corroles and their photochemical decomposition products. J Mass Spectrom 45:1443–1451
37. Wu D, Xu G, Qu S, Xue R, Gu C, Zhang F (1989) Standard enthalpies of combustion and formation of porphyrin derivatives. Thermochim Acta 154:233–245
38. Patiño R, Campos M, Torres LA (2007) Strength of the Zn–N coordination bond in zinc porphyrins on the basis of experimental thermochemistry. Inorg Chem 46:9332–9336
39. Gamboa M, Campos M, Torres LA (2010) Study of the stability of 5,10,15,20-tetraphenylporphine (TPP) and metalloporphyrins NiTPP, CoTPP, CuTPP, and ZnTPP by differential scanning calorimetry and thermogravimetry. J Chem Thermodyn 42:666–674
40. Antina EV, Balantseva EV, Berezin MB (2011) Oxidative degradation of porphyrins and metalloporphyrins under polythermal conditions. Russ J Gen Chem 81:1222–1230
41. Gokakakar SD, Salker AV (2010) Thermal studies of cobalt, iron and tin metalloporphyrins. J Therm Anal Calorim 101:809–813
42. Bonnett R, Stephenson GF (1965) The *meso* reactivity of porphyrins and related compounds. I. Nitration. J Org Chem 30:2791–2798
43. Bonnett R, Dimsdale MJ (1968) The *meso*-hydroxylation and *meso*-benzoxylation of pyridine octaethylhaemochrome. Tetrahedron Lett 9:731–733

44. Bonnett R, Dimsdale MJ, Stephenson GF (1969) The *meso*-reactivity of porphyrins and related compounds. Part IV. Introduction of oxygen functions. J Chem Soc (C) 564–570
45. Bonnett R, Dimsdale MJ (1972) The *meso*-reactivity of porphyrins and related compounds. Part V. The *meso*-oxidation of metalloporphyrins. J Chem Soc Perkin Trans 1 2540–2548
46. Bonnett R, Cornell P, McDonagh AF (1976) The *meso*-reactivity of porphyrins and related compounds. Part VII. Benzoyloxylation of phenylpyrroles and of octaethylporphyrin. J Chem Soc Perkin Trans 1 794–800
47. Smith KM (1971) Reactions of porphyrins with thallium(III) trifluoroacetate. Chem Commun 540–541
48. Cavaleiro JAS, Smith KM (1971) Reactions of *trans*-octaethylchlorin with thallium(III) trifluoroacetate. Chem Commun 1384–1385
49. McCombie SW, Smith KM (1972) Oxophlorin (oxyporphyrin) synthesis. Tetrahedron Lett 13:2463–2464
50. Barnett GH, Hudson MF, McCombie SW, Smith KM (1973) Synthesis of oxophlorins (oxyporphyrins) from magnesium and zinc porphyrin chelates. J Chem Soc Perkin Trans 1 691–696
51. Evans B, Smith KM, Cavaleiro JAS (1976) Ring cleavage of *meso*-tetraphenylporphyrin. Tetrahedron Lett 17:4863–4866
52. Evans B, Smith KM, Cavaleiro JAS (1978) Bile pigment studies. Part 4. Some novel reactions of metalloporphyrins with thallium(III) and cerium(IV) salts. Ring cleavage of *meso*-tetraphenylporphyrin. J Chem Soc Perkin Trans 1 768–773
53. Huster MS, Smith KM (1988) Ring cleavage of chlorophyll derivatives: isolation of oxochlorin intermediates and ring opening via a two oxygen molecule mechanism. Tetrahedron Lett 29:5707–5710
54. Kalish HR, Latos-Grażyński L, Balch AL (2000) Heme/hydrogen peroxide reactivity: formation of paramagnetic iron oxophlorin isomers by treatment of iron porphyrins with hydrogen peroxide. J Am Chem Soc 122:12478–12486
55. Kalish H, Camp JE, Stępień M, Latos-Grażyński L, Balch AL (2001) Reactivity of mono-*meso*-substituted iron(II) octaethylporphyrin complexes with hydrogen peroxide in the absence of dioxygen. Evidence for nucleophilic attack on the heme. J Am Chem Soc 123:11719–11727
56. Wojaczyński J, Latos-Grażyński L, Chmielewski PJ, Van Calcar P, Balch AL (1999) ^{1}H NMR investigations of triphenylporphyrin metal complexes and electronic interactions in iron(III) complexes of *meso–meso*-linked 5,5′-bis(10,15,20-triphenylporphyrin). Inorg Chem 38:3040–3050
57. Osuka A, Shimidzu H (1997) meso, meso-Linked porphyrin arrays. Angew Chem Int Ed Engl 36:135–137
58. Yoshida N, Shimidzu K, Osuka A (1998) *meso-meso* Linked diporphyrins from 5,10,15-trisubstituted porphyrins. Chem Lett 27:55–56
59. Yoshida N, Aratani N, Osuka A (2000) Poly(zinc(II)-5,15-porphyrinylene) from silver(I)-promoted oxidation of zinc(II)-5,15-diarylporphyrins. Chem Commun 197–198
60. Catalano MM, Crossley MJ, Harding MM, King LG (1984) Control of reactivity at the porphyrin periphery by metal ion co-ordination: a general method for specific nitration at the β-pyrrolic position of 5,10,15,20-tetraarylporphyrins. J Chem Soc Chem Commun 1535–1536
61. Shine HJ, Padilla AG, Wu S-M (1979) Ion radicals. 45. Reactions of zinc tetraphenylporphyrin cation radical perchlorate with nucleophiles. J Org Chem 44:4069–4075
62. Abhilash GJ, Bhuyan J, Singh P, Maji S, Pal K, Sarkar S (2009) $^{\bullet}NO_2$-mediated *meso*-hydroxylation of iron(III) porphyrin. Inorg Chem 48:1790–1792
63. Bhuyan J, Sarkar S (2010) Oxidative degradation of zinc porphyrin in comparison with its iron analogue. Chem Eur J 16:10649–10652
64. Ongayi O, Fronczek FR, Vicente MGH (2003) Benzoylbiliverdins from chemical oxidation of dodeca-substituted porphyrins. Chem Commun 2298–2299

65. Ongayi O, Vicente MGH, Ou Z, Kadish KM, Kumar MR, Fronczek FR, Smith KM (2006) Synthesis and electrochemistry of undeca-substituted metallo-benzoylbiliverdins. Inorg Chem 45:1463–1470
66. Ongayi O, Vicente MGH, Ghosh B, Fronczek FR, Smith KM (2010) Bilitrienones from the chemical oxidation of dodecasubstituted porphyrins. Tetrahedron 66:63–67
67. Ponomarev GV, Morozova YV, Yashunsky DV (2001) Chemistry of oximes of *meso*-formylporphyrins. Opening of the porphyrin macrocycle into tripyrrolylisoxazoles. The revised structure of "isophlorins". Chem Heterocycl Compd 37:253–255
68. Morozova YV, Nesterov VV, Yashunsky DV, Antipin MY, Ponomarev GV (2005) Porphyrins. 40. Chemistry of oximes of metal complexes of *meso*-formyloctaalkylporphyrins. Synthesis, molecular and crystal structure of nickel complexes of "tripyrrolylisoxazoles". Chem Heterocycl Compd 41:598–605
69. Kalish H, Lee HM, Olmstead MM, Latos-Grażyński L, Rath SP, Balch AL (2003) Heme cleavage with remarkable ease: paramagnetic intermediates formed by aerobic oxidation of a *meso*-amino-substituted iron porphyrin. J Am Chem Soc 125:4674–4675
70. Rath SP, Kalish H, Latos-Grażyński L, Olmstead MM, Balch AL (2004) Facile ring opening of iron(III) and iron(II) complexes of *meso*-amino-octaethylporphyrin by dioxygen. J Am Chem Soc 126:646–654
71. Sprutta N, Rath SP, Olmstead MM, Balch AL (2005) Metal complexes of *meso*-amino-octaethylporphyrin and the oxidation of Ni^{II}(*meso*-amino-octaethylporphyrin). Inorg Chem 44:1452–1459
72. Chang CK, Avilés G, Bag N (1994) Verdoheme-like oxaporphyrin formation by oxygenation of a Co(II) porphyrinyl naphthoic acid. A new model of heme degradation. J Am Chem Soc 116:12127–12128
73. Yamanishi K, Miyazawa M, Yairi T, Sakai S, Nishina N, Kobori Y, Kondo M, Uchida F (2011) Conversion of cobalt(II) porphyrin into a helical cobalt(III) complex of acyclic pentapyrrole. Angew Chem Int Ed 50:6583–6586
74. Liu C, Shen D-M, Chen Q-Y (2006) Unexpected bromination ring-opening of tetraarylporphyrins. Chem Commun 770–772
75. Meunier B (1992) Metalloporphyrins as versatile catalysts for oxidation reactions and oxidative DNA cleavage. Chem Rev 92:1411–1456
76. Che C-M, Huang J-S (2009) Metalloporphyrin-based oxidation systems: from biomimetic reactions to application in organic synthesis. Chem Commun 3996–4015
77. Lu H, Zhang XP (2011) Catalytic C–H functionalization by metalloporphyrins: recent developments and future directions. Chem Soc Rev 40:1899–1909
78. Mansuy D (2007) A brief history of the contribution of metalloporphyrin models to cytochrome P450 chemistry and oxidation catalysis. C R Chim 10:392–413
79. Traylor PS, Dolphin D, Traylor TG (1984) Sterically protected hemins with electronegative substituents: efficient catalysts for hydroxylation and epoxidation. J Chem Soc Chem Commun 279–280
80. Banfi S, Montanari F, Quici S (1988) New manganese tetrakis(halogenoaryl)porphyrins featuring sterically hindering electronegative substituents: synthesis of highly stable catalysts in olefin epoxidation. J Org Chem 53:2863–2866
81. Moore KT, Horváth IT, Therien MJ (1997) High-pressure NMR studies of (porphinato)iron-catalyzed isobutane oxidation utilizing dioxygen as the stoichiometric oxidant. J Am Chem Soc 119:1791–1792
82. Leanord DR, Lindsay Smith JR (1991) Model systems for cytochrome P450 dependent monooxygenases. Part 8. A study of the epoxidation of (*Z*)-cyclooctene by iodosylbenzene catalysed by cationic iron(III) tetra(*N*-methylpyridyl)porphyrins adsorbed on Dowex MSC1. J Chem Soc Perkin Trans 2 25–30
83. Nappa MJ, Tolman CA (1985) Steric and electronic control of iron porphyrin catalyzed hydrocarbon oxidations. Inorg Chem 24:4711–4719

84. Pietzyk B, Fröhlich L, Göber B (1995) Characterization and stability of synthetic porphyrins. Pharmazie 50:747–750
85. Pietzyk B, Fröhlich L, Göber B (1996) Stability of synthetic Mn- and Fe-tetraphenylporphyrins in biomimetic systems of aromatic hydroxylation. Pharmazie 51:654–660
86. Stephenson NA, Bell AT (2005) A study of the mechanism and kinetics of cyclooctene epoxidation catalyzed by iron(III) tetrakispentafluorophenyl porphyrin. J Am Chem Soc 127:8635–8643
87. Stephenson NA, Bell AT (2007) Mechanistic insights into iron porphyrin-catalyzed olefin epoxidation by hydrogen peroxide: factors controlling activity and selectivity. J Mol Catal A Chem 275:54–62
88. Cunningham ID, Danks TN, O'Connell KTA, Scott PW (1999) Kinetics and mechanism of the hydrogen peroxide oxidation of a pentafluorophenyl-substituted iron(III) porphyrin. J Chem Soc Perkin Trans 2 2133–2139
89. Cunningham ID, Danks TN, Hay JN, Hamerton I, Gunathilagan S (2001) Evidence for parallel destructive, and competitive epoxidation and dismutation pathways in metalloporphyrin-catalysed alkene oxidation by hydrogen peroxide. Tetrahedron 57:6847–6853
90. Cunningham ID, Danks TN, Hay JN, Hamerton I, Gunathilagan S, Janczak C (2002) Stability of various metalloporphyrin catalysts during hydrogen peroxide epoxidation of alkene. J Mol Catal A Chem 185:25–31
91. Serra AC, Marçalo EC, Rocha Gonsalves AM'A (2004) A view on the mechanism of metalloporphyrin degradation in hydrogen peroxide epoxidation reactions. J Mol Catal A Chem 215:17–21
92. Rácz K, Burger M, Ungvarai-Nagy Z (2010) Comparison of the oxidation of two porphyrin complexes by bromate with respect to wave propagation. Physica D 239:752–756
93. Rácz K, Burger M, Nagy-Ungvarai Z (2006) Autocatalytic oxidation of hemin by acidic bromate. Int J Chem Kinet 38:503–509
94. Rácz K, Burger M, Lagzi I, Ungvarai-Nagy Z (2008) Oxidation of a water-soluble porphyrin complex by bromate. React Kinet Catal Lett 95:135–142
95. Türk H, Erdem M (2004) Structural stabilities of *N*-permethylated tetracations of *meso*-tetrakis(4-pyridyl)porphyrin, *meso*-tetrakis[4-(dimethylamino)phenyl]porphyrin and their manganese(III) complexes toward hydrogen peroxide, *tert*-butylhydroperoxide and sodium hypochlorite. J Porphyr Phthalocyanines 8:1196–1203
96. Türk H, Tay T, Berber H (2000) Structural stabilities of sulfonated manganese tetramesitylporphyrin and its β-brominated analogue toward NaOCl, H_2O_2 and $(CH_3)_3COOH$. J Mol Catal A Chem 160:323–330
97. Türk H, Berber H (2000) Structural stabilities of water-soluble MnTDCSPP, MnTSPP, and supported analogues toward hydrogen peroxide and sodium hypochlorite. Int J Chem Kinet 32:271–278
98. Türk H, Berber H (2001) Structural studies of water-soluble β-brominated manganese porphyrins: stabilities of $MnTDCSPPBr_8$ and $MnTSPPBr_8$ as homogeneous and supported reagents toward hydrogen peroxide and sodium hypochlorite. Turk J Chem 25:215–222
99. Lente G, Fábián I (2007) Kinetics and mechanism of the oxidation of water soluble porphyrin $Fe^{III}TPPS$ with hydrogen peroxide and the peroxomonosulfate ion. Dalton Trans 4268–4275
100. Chmielewski PJ, Latos-Grażyński L, Rachlewicz K, Głowiak T (1994) Tetra-*p*-tolylporphyrin with an inverted pyrrole ring: a novel isomer of porphyrin. Angew Chem Int Ed Engl 33:779–781
101. Furuta H, Asano T, Ogawa T (1994) "N-confused porphyrin": a new isomer of tetraphenylporphyrin. J Am Chem Soc 11:767–768
102. Furuta H, Maeda H, Osuka A (2002) Regioselective oxidative liberation of aryl-substituted tripyrrinone metal complexes from N-confused porphyrin. Org Lett 4:181–184
103. Furuta H, Maeda H, Osuka A (2003) Crystal structures of palladium(II) and copper(II) complexes of *meso*-phenyl tripyrrinone. Inorg Chem Commun 6:162–164

104. Pawlicki M, Kańska I, Latos-Grażyński L (2007) Copper(II) and copper(III) complexes of pyrrole-appended oxacarbaporphyrin. Inorg Chem 46:6575–6584
105. Lemon CM, Brothers PJ (2011) The synthesis reactivity and peripheral functionalization of corroles. J Porphyr Phthalocyanines 15:809–834
106. Nardis S, Mandoj F, Paolesse R, Fronczek FR, Smith KM, Prodi L, Montalti M, Battistini G (2007) Synthesis and functionalization of germanium triphenylcorrolate: the first example of a partially brominated corrole. Eur J Inorg Chem 2345–2352
107. Mandoj F, Nardis S, Pomarico G, Stefanelli M, Schiaffino L, Ercolani G, Prodi L, Genovese D, Zaccheroni N, Fronczek FR, Smith KM, Xiao X, Shen J, Kadish KM, Paolesse R (2009) 6-Azahemiporphycene: a new member of the porphyrinoid family. Inorg Chem 8:10346–10357
108. Gros CP, Barbe J-M, Espinosa E, Guilard R (2006) Room-temperature autoconversion of free-base corrole into free-base porphyrin. Angew Chem Int Ed 45:5642–5645
109. Nardis S, Pomarico G, Fronczek FR, Vicente MGH, Paolesse R (2007) One-step synthesis of isocorroles. Tetrahedron Lett 48:8643–8646
110. Pomarico G, Xiao X, Nardis S, Paolesse R, Fronczek FR, Smith KM, Fang Y, Ou Z, Kadish KM (2010) Synthesis and characterization of free-base copper, and nickel isocorroles. Inorg Chem 49:5766–5774
111. Mandoj F, Nardis S, Pomarico G, Paolesse R (2008) Demetalation of corrole complexes: an old dream turning into reality. J Porphyr Phthalocyanines 12:19–26
112. Stefanelli M, Shen J, Zhu W, Mastroianni M, Mandoj F, Nardis S, Ou Z, Kadish KM, Fronczek FR, Smith KM, Paolesse R (2009) Demetalation of silver(III) corrolates. Inorg Chem 48:6879–6887
113. Barata JFB, Silva AMG, Neves MGPMS, Tomé AC, Silva AMS, Cavaleiro JAS (2006) β,β′-Corrole dimers. Tetrahedron Lett 47:8171–8174
114. Bonnett R, Martínez G (2001) Photobleaching of sensitisers used in photodynamic therapy. Tetrahedron 57:9513–9547
115. Wöhrle D, Wendt A, Weitmeyer A, Stark J, Spiller W, Schneider G, Müller S, Michelsen U, Kliesch H, Heuermann A, Ardeschirpur A (1994) Metal chelates of porphyrin derivatives as sensitizers in photooxidation processes of sulfur compounds and in photodynamic therapy of cancer. Russ Chem Bull 43:1953–1964
116. Silva M, Azenha ME, Pereira MM, Burrows HD, Sarakha M, Forano C, Ribeiro MF, Fernandes A (2010) Immobilization of halogenated porphyrins and their copper complexes in MCM-41: environmentally friendly photocatalysts for the degradation of pesticides. Appl Catal B 100:1–9
117. Kim H, Kim W, Mackeyev Y, Lee G-S, Kim H-J, Tachikawa T, Hong S, Lee S, Kim J, Wilson LJ, Majima T, Alvarez PJJ, Choi W, Lee J (2012) Selective oxidative degradation of organic pollutants by singlet oxygen-mediated photosensitization: tin porphyrin versus C_{60} aminofullerene systems. Environ Sci Technol 46:9606–9613
118. Sternberg ED, Dolphin D, Brückner C (1998) Porphyrin-based photosensitizers for use in photodynamic therapy. Tetrahedron 54:4151–4202
119. Ali H, van Lier JE (2010) Porphyrins and phthalocyanines as photosensitizers and radiosensitizers. In: Kadish KM, Smith KM, Guilard R (eds) Handbook of porphyrin science with applications to chemistry, physics, materials science, engineering biology and medicine, vol 4. World Scientific, Singapore, pp 1–119 (Chapter 16)
120. Arnaut LG (2011) Design of porphyrin-based photosensitizers for photodynamic therapy. Adv Inorg Chem 63:187–233
121. Ethirajan M, Chen Y, Joshi P, Pandey RK (2011) The role of porphyrin chemistry in tumor imaging and photodynamic therapy. Chem Soc Rev 40:340–362
122. Fuhrhop J-H, Mauzerall D (1971) The photooxygenation of magnesium-octaethylporphin. Photochem Photobiol 13:453–458
123. Bonnett R, Chaney BD (1987) *meso*-Reactivity of porphyrins and related compounds. Part 9. Photo-oxygenation of octaethyloxophlorin. J Chem Soc Perkin Trans 1 1063–1067

124. Matsuura T, Inoue K, Ranade AC, Saito I (1980) Photooxygenation of magnesium *meso*-tetraphenylporphyrin. Photochem Photobiol 31:23–26
125. Smith KM, Brown SB, Troxler RF, Lai J-J (1982) Photooxygenation of *meso*-tetraphenylporphyrin metal complexes. Photochem Photobiol 36:147–152
126. Smith KM, Brown SB, Troxler RF, Lai J-J (1980) Mechanism of photo-oxygenation of *meso*-tetraphenylporphyrin metal complexes. Tetrahedron Lett 21:2763–2766
127. Cavaleiro JAS, Hewlins MJE, Jackson AH, Neves GPMS (1986) Structures of the ring-opened oxidation products from *meso*-tetraphenylporphyrin. J Chem Soc Chem Commun 142–144
128. Cavaleiro JAS, Neves MGPS, Hewlins MJE, Jackson AH (1990) The photo-oxidation of meso-tetraphenylporphyrins. J Chem Soc Perkin Trans 1 1937–1943
129. Silva AMS, Neves MGPMS, Martins RRL, Cavaleiro JAS, Boschi T, Tagliatesta P (1998) Photo-oxygenation of *meso*-tetraphenylporphyrin derivatives: the influence of the substitution pattern and characterization of the reaction products. J Porphyr Phthalocyanines 2:45–51
130. Cavaleiro JAS, Hewlins MJE, Jackson AH, Neves MGPMS (1992) Structures of the zinc complexes of the bilinones formed by photo-oxidations of *meso*-tetraphenylporphyrins. Tetrahedron Lett 33:6871–6874
131. Jeandon C, Krattinger B, Ruppert R, Callot HJ (2001) Biladienones from the photooxidation of a *meso-gem*-disubstituted phlorin: crystal and molecular structures of the 3N + O coordinated nickel(II) and copper(II) complexes. Inorg Chem 40:3149–3153
132. LeSaulnier TD, Graham BW, Geier GR III (2005) Enhancement of phlorin stability by the incorporation of *meso*-mesityl substituents. Tetrahedron Lett 46:5633–5637
133. Herath HMA, Karunaratne V, Rajapakse RMG, Wickramasinghe A (2005) Synthesis, characterization and photochemistry of 5,10,15,20-tetrakis(4-*N*-pentylpyridyl)porphyrins, $[(TPePyP)H_2]^{4+}$ and $[(TPePyP)Zn^{II}]^{4+}$. J Porphyr Phthalocyanines 9:155–162
134. Niziolek M, Korytowski W, Girotti AW (2005) Self-sensitized photodegradation of membrane-bound protoporphyrin mediated by chain lipid peroxidation: inhibition by nitric oxide with sustained singlet oxygen damage. Photochem Photobiol 81:299–305
135. Cavaleiro JAS, Görner H, Lacerda PSS, MacDonald JG, Mark G, Neves MGPMS, Nohr RS, Schuchmann H-P, von Sonntag C, Tomé AC (2001) Singlet oxygen formation and photostability of *meso*-tetraarylporphyrin derivatives and their copper complexes. J Photochem Photobiol A Chem 144:131–140
136. Wojaczyński J, Latos-Grażyński L (2010) Photooxidation of N-confused porphyrin: a route to N-confused biliverdin analogues. Chem Eur J 16:2679–2682
137. Wojaczyński J, Popiel M, Szterenberg L, Latos-Grażyński L (2011) Common origin, common fate: regular porphyrin and N-confused porphyrin yield an identical tetrapyrrolic degradation product. J Org Chem 76:9956–9961
138. Aviv I, Gross Z (2007) Corrole-based applications. Chem Commun 1987–1999
139. Flamigni L, Gryko DT (2009) Photoactive corrole-based arrays. Chem Soc Rev 38:1635–1646
140. Ventura B, Degli Esposti A, Koszarna B, Gryko DT, Flamigni L (2005) Photophysical characterization of free-base corroles, promising chromophores for light energy conversion and singlet oxygen generation. New J Chem 9:1559–1566
141. Geier GR III, Chick JFB, Callinan JB, Reid CG, Auguscinski WP (2004) A survey of acid catalysis and oxidation conditions in the two-step one-flask synthesis of *meso*-substituted corroles via dipyrromethanedicarbinols and pyrrole. J Org Chem 69:4159–4169
142. Ding T, Alemán EA, Modarelli DA, Ziegler CJ (2005) Photophysical properties of a series of free-base corroles. J Phys Chem A 109:7411–7417
143. Tardieux C, Gros CP, Guilard R (1998) On corrole chemistry. An isomerization and oxidative cleavage of the corrole macroring to a biliverdin structure. J Heterocycl Chem 35:965–970
144. Paolesse R, Sagone F, Macagnano A, Boschi T, Prodi L, Montalti M, Zaccheroni N, Bolletta F, Smith KM (1999) Photophysical behaviour of corrole and its symmetrical and unsymmetrical dyads. J Porphyr Phthalocyanines 3:364–370

145. Yamauchi T, Mizutani T, Wada K, Horii S, Furukawa H, Masaoka S, Chang H-C, Kitagawa S (2005) A facile and versatile preparation of bilindiones and biladienones from tetraarylporphyrins. Chem Commun 1309–1311
146. Jérôme F, Gros CP, Tardieux C, Barbe J-M, Guilard R (1998) First synthesis of sterically hindered cofacial bis(corroles) and their bis(cobalt) complexes. Chem Commun 2007–2008
147. Wojaczyński J, Duszak M, Latos-Grażyński L (unpublished results)
148. Barata JFB, Neves MGPMS, Tomé AC, Faustino MAF, Silva AMS, Cavaleiro JAS (2010) How light affects 5,10,15-tris(pentafluorophenyl)corrole. Tetrahedron Lett 51:1537–1540
149. Warburg O, Negelein E (1930) Grünes Haemin aus Blut-Haemin. Chem Ber 63:1816–1818
150. Lemberg R (1956) Chemical mechanism of bile pigment formation. Rev Pure Appl Chem 6:1–23
151. Lemberg R, Cortis-Jones B, Norrie M (1937) Coupled oxidation of ascorbic acid and haemochromogens. Nature 139:1016–1017
152. Libowitzky H, Fischer H (1938) Bile pigments. XVIII. From coprohemin I to coproglaucobilin. Z Physiol Chem 255:209–233
153. Balch AL, Latos-Grażyński L, Noll BC, Olmstead MM, Szterenberg L, Safari N (1993) Structural characterization of verdoheme analogs. Iron complexes of octaethyloxoporphyrin. J Am Chem Soc 115:1422–1429
154. Balch AL, Latos-Grażyński L, Noll BC, Olmstead MM, Safari N (1993) Isolation and characterization of an iron biliverdin-type complex that is formed along with verdohemochrome during the coupled oxidation of iron(II) octaethylporphyrin. J Am Chem Soc 115:9056–9061
155. St Claire TN, Balch AL (1999) In situ monitoring of the degradation of iron porphyrins by dioxygen with hydrazine as sacrificial reductant. Detection of paramagnetic intermediates in the coupled oxidation process by ^{1}H NMR spectroscopy. Inorg Chem 38:684–691
156. Balch AL, Koerner R, Latos-Grażyński L, Lewis JE, St Claire TN, Zovinka EP (1997) Coupled oxidation of heme without pyridine. Formation of cyano complexes of iron oxophlorin and 5-oxaporphyrin (verdoheme) from octaethylheme. Inorg Chem 36:3892–3897
157. Balch AL, Mazzanti M, St Claire TN, Olmstead MM (1995) Production of oxaporphyrin and biliverdin derivatives by coupled oxidation of cobalt(II) octaethylporphyrin. Inorg Chem 34:2194–2200
158. Wojaczyński J, Stępień M, Latos-Grażyński L (2002) Monomeric and dimeric iron(III) complexes of 5-hydroxy-10,15,20-triphenylporphyrin: formation of cyano and pyridine complexes of (5-oxo-10,15,20-triphenylphlorin)iron. Eur J Inorg Chem 1806–1815
159. Asano N, Uemura S, Kinugawa T, Akasaka H, Mizutani T (2007) Synthesis of biladienone and bilatrienone by coupled oxidation of tetraarylporphyrins. J Org Chem 72:5320–5326
160. Nakamura R, Kakeya K, Furuta N, Muta E, Nishisaka H, Mizutani T (2011) Synthesis of *para*- or *ortho*-substituted triarylbilindiones and tetraarylbiladienones by coupled oxidation of tetraarylporphyrins. J Org Chem 76:6108–6115
161. Balch AL (2000) Coordination chemistry with *meso*-hydroxylated porphyrins (oxophlorins), intermediates in heme degradation. Coord Chem Rev 200–202:349–377
162. Balch AL, Latos-Grażyński L, Noll BC, Olmstead MM, Zovinka EP (1992) Chemistry of iron oxophlorins. 1. ^{1}H NMR and structural studies of five-coordinate iron(III) complexes. Inorg Chem 31:2248–2255
163. Balch AL, Noll BC, Zovinka EP (1992) Structural characterization of zinc(II) complexes of octaethyloxophlorin dianion and octaethyloxophlorin radical anion. J Am Chem Soc 114:3380–3385
164. Balch AL, Noll BC, Phillips SL, Reid SM, Zovinka EP (1993) Nickel(II) complexes of the octaethyloxophlorin dianion and octaethyloxophlorin radical dianion. Inorg Chem 32:4730–4736

165. Balch AL, Noll BC, Reid SM, Zovinka EP (1993) Coordination patterns for oxophlorin ligands. Pyridine-induced cleavage of dimeric manganese(III) and iron(III) octaethyloxophlorin complexes. Inorg Chem 32:2610–2611
166. Balch AL, Mazzanti M, Olmstead MM (1993) Cobalt complexes of octaethyloxophlorin. Metal-centered redox chemistry in the presence of a redox-active ligand. Inorg Chem 32:4737–4744
167. Masuoka N, Itano HA (1987) Radical intermediates in the oxidation of octaethylheme to octaethylverdoheme. Biochemistry 26:3672–3680
168. Balch AL, Latos-Grażyński L, Noll BC, Szterenberg L, Zovinka EP (1993) Chemistry of iron oxophlorins. 2. Oxidation of the iron(III) octaethyloxophlorin dimer and observation of stepwise two-electron oxidation of the oxophlorin macrocycle. J Am Chem Soc 115:11846–11854
169. Balch AL, Noll BC, Olmstead MM, Reid SM (1993) A cofacial dimeric, metallooxophlorin complex: [indium(III)(octaethyloxophlorin)]$_2$. J Chem Soc Chem Commun 1088–1090
170. Balch AL, Latos-Grażyński L, St Claire TN (1995) Chemistry of iron oxophlorins. 3. Reversible, one-electron oxidation of the iron(III) octaethyloxophlorin dimer. Inorg Chem 34:1395–1401
171. Garcia TY, Olmstead MM, Fettinger JC, Balch AL (2008) Cleavage of the indium(III) octaethyloxophlorin dimer, {In^{III}(OEPO)}$_2$, with Lewis bases. Importance of outer-sphere hydrogen bonding in adduct structures. Inorg Chem 47:11417–11422
172. Sano S, Sugiura Y, Meada Y, Ogawa S, Morishima I (1981) Electronic states of iron oxyporphyrin and verdohemochrome obtained by coupled oxidation of iron porphyrin. J Am Chem Soc 103:2888–2890
173. Morishima I, Fujii H, Shiro Y, Sano S (1986) NMR studies of metalloporphyrin radicals. Iron (II) oxophlorin radical formed from iron(III) *meso*-hydroxyoctaethylporphyrin. J Am Chem Soc 108:3858–3860
174. Morishima I, Fujii H, Shiro Y, Sano S (1995) Studies on the iron(II) *meso*-oxyporphyrin π-neutral radical as a reaction intermediate in heme catabolism. Inorg Chem 34:1528–1535
175. Balch AL, Koerner R, Noll BC (1996) A role for electron transfer in heme catabolism? Structure and redox behavior of an intermediate, (pyridine)$_2$Fe(octaethyloxophlorin). J Am Chem Soc 118:2760–2761
176. Szterenberg L, Latos-Grażyński L, Wojaczyński J (2002) Oxophlorin and metallooxophlorin radicals − DFT studies. Chemphyschem 3:575–583
177. Rath SP, Olmstead MM, Balch AL (2004) The effects of axial ligands on electron distribution and spin states in iron complexes of octaethyloxophlorin, intermediates in heme degradation. J Am Chem Soc 126:6379–6386
178. Rath SP, Olmstead MM, Balch AL (2006) Electron distribution in iron octaethyloxophlorin complexes. Importance of the Fe(III) oxophlorin trianion form in the bis-pyridine and bis-imidazole complexes. Inorg Chem 45:6083–6093
179. Gheidi M, Safari N, Zahedi M (2012) Effect of axial ligand on the electronic configuration, spin states, and reactivity of iron oxophlorin. Inorg Chem 51:7094–7102
180. Rath SP, Koerner R, Olmstead MM, Balch AL (2003) Reversible binding of nitric oxide and carbon–carbon bond formation in a *meso*-hydroxylated heme. J Am Chem Soc 125:11798–11799
181. Rath SP, Olmstead MM, Balch AL (2004) Reactions of *meso*-hydroxyhemes with carbon monoxide and reducing agents in search of the elusive species responsible for the $g = 2.006$ resonance of carbon monoxide-treated heme oxygenase. Isolation of diamagnetic iron(II) complexes of octaethyl-*meso*-hydroxyporphyrin. Inorg Chem 43:6357–6365
182. Rath SP, Olmstead MM, Latos-Grażyński L, Balch AL (2003) Formation and isolation of an iron-tripyrrole complex from heme degradation. J Am Chem Soc 125:12678–12679
183. Ortiz de Montellano PR, Auclair K (2003)) Heme oxygenase structure and mechanism. In: Kadish KM, Smith KM, Guilard R (eds) The porphyrin handbook, vol 12. Academic, San Diego, pp 183–210 (Chapter 75)

184. Saito S, Itano HA (1986) Cyclization of biliverdins to verdohaemochromes. J Chem Soc Perkin Trans 1 1–7
185. Saito S, Sumita S, Iwai K, Sano H (1988) Preparation of mesoverdohemochrome IXα dimethyl ester and Mössbauer spectra of related porphyrins. Bull Chem Soc Jpn 61:3539–3547
186. Balch AL, Noll BC, Safari N (1993) Structural characterization of low-spin iron(III) complexes of octaethyloxoporphyrin. Inorg Chem 32:2901–2905
187. Balch AL, Mazzanti M, Olmstead MM (1994) Preparation of a cobalt analogue of verdoheme by coupled oxidation of cobalt(II) octaethylporphyrin. J Chem Soc Chem Commun 269–270
188. Balch AL, Koerner R, Olmstead MM (1995) Crystallographic characterization of octaethylverdohaem. J Chem Soc Chem Commun 873–874
189. Lord PA, Latos-Grażyński L, Balch AL (2002) Reactivity of iron verdohemes with phenylmagnesium bromide. Formation of paramagnetic iron–phenyl complexes. Inorg Chem 41:1011–1014
190. Rath SP, Olmstead MM, Balch AL (2004) Oxidative verdoheme formation and stabilization by axial isocyanide ligation. Inorg Chem 43:7648–7655
191. Khorasani-Motlagh M, Safari N, Noroozifar M, Saffari J, Biabani M, Rebouças JS, Patrick BO (2005) New class of verdoheme analogues with weakly coordinating anions: the structure of (μ-oxo)bis[(octaethyloxoporphinato)iron(III)] hexafluorophosphate. Inorg Chem 44:7762–7769
192. Khorasani-Motlagh M, Safari N, Noroozifar M, Shahroosvand H, Parsaii Z, Patrick BO (2007) Formation and stabilization of five-coordinate iron(II) verdoheme analogues by axial weakly coordinating anion ligation. X-ray crystal structures of $[(OEOPFe)_2O](X)_2$ ($X = AsF_6$, SbF_6). Inorg Chim Acta 360:2331–2338
193. Balch AL, Bowles FL (2010)) Coordination chemistry of verdohemes and open-chain oligopyrrole systems involved in heme oxidation and porphyrin destruction. In: Kadish KM, Smith KM, Guilard R (eds) Handbook of porphyrin science with applications to chemistry, physics, materials science, engineering biology and medicine, vol 8. World Scientific, Singapore, pp 293–342 (Chapter 40)
194. Saito S, Itano HA (1982) Verdohemochrome IXα: preparation and oxidoreductive cleavage to biliverdin IXα. Proc Natl Acad Sci USA 79:1393–1397
195. Nguyen KT, Rath SP, Latos-Grażyński L, Olmstead MM, Balch AL (2004) Formation of a highly oxidized iron biliverdin complex upon treatment of a five-coordinate verdoheme with dioxygen. J Am Chem Soc 126:6210–6211
196. Fuhrhop J-H, Krüger P (1977) 1-Oder 19-methoxy-1-oder 19-amino-und 1-oder 19-thiodesoxybiliverdine. Liebigs Ann 360–370
197. Latos-Grażyński L, Johnson J, Attar S, Olmstead MM, Balch AL (1998) Reactivity of the verdoheme analogues, 5-oxaporphyrin complexes of cobalt(II) and zinc(II) with nucleophiles: opening of the planar macrocycle by alkoxide addition to form helical complexes. Inorg Chem 37:4493–4499
198. Koerner R, Latos-Grażyński L, Balch AL (1998) Models for verdoheme hydrolysis. Paramagnetic products from the ring opening of verdohemes, 5-oxaporphyrin complexes of iron(II) with methoxide ion. J Am Chem Soc 120:9246–9255
199. Johnson JA, Olmstead MM, Stolzenberg AM, Balch AL (2001) Ring-opening and *meso* substitution from the reaction of cyanide ion with zinc verdohemes. Inorg Chem 40:5585–5595
200. Latos-Grażyński L, Wojaczyński J, Koerner R, Johnson JJ, Balch AL (2001) Verdoheme reactivity. Remarkable paramagnetically shifted ^{1}H NMR spectra of intermediates from the addition of hydroxide or methoxide with Fe^{II} and Fe^{III} verdohemes. Inorg Chem 40:4971–4977
201. Johnson JA, Olmstead MM, Balch AL (1999) Reactivity of the verdoheme analogues. Opening of the planar macrocycle by amide and thiolate nucleophiles to form helical complexes. Inorg Chem 38:5379–5383

202. Saito S, Itano HA (1987) Autoxidation and solvolysis products of octaethylverdohaemochrome. J Chem Soc Perkin Trans 1 1183–1188
203. Davari MD, Bahrami H, Zahedi M, Safari N (2010) Effect of the axial ligands on the structure and reactivity of tin verdoheme in the ring opening process. Inorg Chim Acta 363:1577–1586
204. Jamaat PR, Safari N, Ghiasi M, Naghavi SS, Zahedi M (2008) Noninnocent effect of axial ligand on the heme degradation process: a theoretical approach to hydrolysis pathway of verdoheme to biliverdin. J Biol Inorg Chem 13:121–132
205. Davari MD, Bahrami H, Zahedi M, Safari N (2009) How tin metal prevents verdoheme ring opening? Comparative study of various nucleophiles. J Mol Struct (THEOCHEM) 908:1–11
206. Davari MD, Bahrami H, Zahedi M, Safari N (2009) Theoretical investigations on the hydrolysis pathway of tin verdoheme complexes: elucidation of tin's ring opening inhibition role. J Mol Model 15:1299–1315
207. Bonfiglio JV, Bonnett R, Hursthouse MB, Malik KMA (1977) Crystal structure of the nickel complex of 2,3,7,8,12,13,17,18-octaethyl-1,19(21*H*,24*H*)-bilindione (octaethylbilatriene-*abc*). J Chem Soc Chem Commun 83–84
208. Bonfiglio JV, Bonnett R, Buckley DG, Hamzetash D, Hursthouse MB, Malik KMA, McDonagh AF, Trotter J (1983) Linear tetrapyrroles as ligands: syntheses and X-ray analyses of boron and nickel complexes of octaethyl-21*H*,24*H*-bilin-1,19-dione. Tetrahedron 39:1865–1874
209. Balch AL, Mazzanti M, Noll BC, Olmstead MM (1993) Geometric and electronic structure and dioxygen sensitivity of the copper complex of octaethylbilindione, a biliverdin analog. J Am Chem Soc 15:12206–12207
210. Balch AL, Mazzanti M, Noll BC, Olmstead MM (1994) Coordination patterns for biliverdin-type ligands. Helical and linked helical units in four-coordinate cobalt and five-coordinate manganese(III) complexes of octaethylbilindione. J Am Chem Soc 116:9114–9122
211. Attar S, Balch AL, Van Calcar PM, Winkler K (1997) Electron transfer behavior and solid state structures of the helical cobalt complexes of the open-chain tetrapyrrole ligand, octaethylbilindione. J Am Chem Soc 119:3317–3323
212. Attar S, Ozarowski A, Van Calcar PM, Winkler K, Balch AL (1997) Axial ligation modulates the electron distribution in helical cobalt complexes derived from octaethylbilindione. Chem Commun 1115–1116
213. Koerner R, Olmstead MM, Van Calcar PM, Winkler K, Balch AL (1998) Carbon monoxide production during the oxygenation of cobalt complexes of linear tetrapyrroles. Formation and characterization of Co^{II}(tetraethylpropentdyopent anion)$_2$. Inorg Chem 37:982–988
214. Lord PA, Olmstead MM, Balch AL (2000) Redox characteristics of nickel and palladium complexes of the open-chain tetrapyrrole octaethylbilindione: a biliverdin model. Inorg Chem 39:1128–1134
215. Lord PA, Noll BC, Olmstead MM, Balch AL (2001) A remarkable skeletal rearrangement of a coordinated tetrapyrrole: chemical consequences of palladium π-coordination to a bilindione. J Am Chem Soc 123:10554–10559
216. Fuhrhop J-H, Krüger P, Sheldrick WS (1977) Darstellung Struktur und Eigenschaften der 5-aza-5-oxonia-und 5-thioniamesoporphin-dimethylester und -protoporphin-dimethylester. Liebigs Ann 339–359
217. Kakeya K, Nakagawa A, Mizutani T, Hitomi Y, Kodera M (2012) Synthesis, reactivity and spectroscopic properties of *meso*-triaryl-5-oxaporphyrins. J Org Chem 77:6510–6519
218. Zahedi M, Bahrami H, Shahbazian S, Safari N, Ng SW (2003) An ab initio/hybrid (ONIOM) investigation of biliverdin isomers and metal–biliverdin analogue complexes. J Mol Struct (THEOCHEM) 633:21–33
219. Wasbotten I, Ghosh A (2006) Biliverdine-based metalloradicals: sterically enhanced noninnocence. Inorg Chem 45:4914–4921
220. Szterenberg L, Latos-Grażyński L, Wojaczyński J (2003) Metallobiliverdin radicals − DFT studies. Chemphyschem 4:691–698

221. Zahedi M, Safari N, Haddadpur S (2000) Semiempirical molecular orbital calculations of biliverdin: study of dynamics and energetics of the self-association of a two-electron oxidation product. J Mol Struct (THEOCHEM) 531:79–88
222. Zahedi M, Kamalipour M, Safari N (2002) Theoretical studies of biliverdin: energetics of the reduction pathways to bilirubin. J Mol Model 8:113–118
223. Bonnett R, McDonagh AF (1970) Oxidative cleavage of the haem system: the four isomeric biliverdins of the IX series. Chem Commun 237–238
224. Bonnett R, McDonagh AF (1973) The *meso*-reactivity of porphyrins and related compounds. Part VI. Oxidative cleavage of the haem system. The four isomeric biliverdins of the IX series. J Chem Soc Perkin Trans 1 881–888
225. Crusats J, Suzuki A, Mizutani T, Ogoshi H (1998) Regioselective porphyrin bridge cleavage controlled by electronic effects. Coupled oxidation of 3-demethyl-3-(trifluoromethyl) mesohemin IX and identification of its four biliverdin derivatives. J Org Chem 63:602–607
226. Niemevz F, Alvarez DE, Buldain GY (2002) Chemical oxidation of synthetic iron(III)-complex of 15-phenyl protoporphyrin IX. Heterocycles 57:697–704
227. Niemevz F, Vazquez MS, Buldain G (2008) Synthesis of a series of mono-*meso*-arylmeso-porphyrins III of biological interest and their biliverdin derivatives. Synthesis 875–882
228. Wang J, Niemevz F, Lad L, Huang L, Alvarez DE, Buldain G, Poulos TL, Ortiz de Montellano PR (2004) Human heme oxygenase oxidation of 5- and 15-phenylhemes. J Biol Chem 279:42593–42604
229. Hudson MF, Smith KM (1975) Bile pigments. Chem Soc Rev 4:363–399
230. Frankenberg N, Lagarias JC (2003)) Biosynthesis and biological functions of bilins. In: Kadish KM, Smith KM, Guilard R (eds) The porphyrin handbook, vol 13. Academic, San Diego, pp 211–235 (Chapter 83)
231. Lagarias JC (1982) Bile pigment-protein interactions. Coupled oxidation of cytochrome c. Biochemistry 21:5962–5967
232. van der Horst MA, Hellingwerf KJ (2004) Photoreceptor proteins "Star actors of modern times": a review of the functional dynamics in the structure of representative members of six different photoreceptor families. Acc Chem Res 37:13–20
233. Tenhunen R, Marver HS, Schmid R (1968) The enzymatic conversion of heme to bilirubin by microsomal heme oxygenase. Proc Natl Acad Sci USA 61:748–755
234. Frydman RB, Frydman B (1987) Heme catabolism: a new look at substrates and enzymes. Acc Chem Res 20:250–256
235. Yoshida T, Migita CT (2000) Mechanism of heme degradation by heme oxygenase. J Inorg Biochem 82:33–41
236. Kikuchi G, Yoshida T, Noguchi M (2005) Heme oxygenase and heme degradation. Biochem Biophys Res Commun 338:558–567
237. Rivera M, Zeng Y (2005) Heme oxygenase steering dioxygen activation toward heme hydroxylation. J Inorg Biochem 99:337–354
238. Morse D, Choi AMK (2005) Heme oxygenase-1. From bench to bedside. Am J Respir Crit Care Med 172:660–670
239. Matsui T, Iwasaki M, Sugiyama R, Unno M, Ikeda-Saito M (2010) Dioxygen activation for the self-degradation of heme: reaction mechanism and regulation of heme oxygenase. Inorg Chem 49:3602–3609
240. Schuller DJ, Zhu W, Stojiljkovic I, Wilks A, Poulos TL (2001) Crystal structure of heme oxygenase from the Gram-negative pathogen *Neisseria meningitidis* and a comparison with mammalian heme oxygenase-1. Biochemistry 40:11552–11558
241. Friedman J, Lad L, Li H, Wilks A, Poulos TL (2004) Structural basis for novel δ-regioselective heme oxygenation in the opportunistic pathogen *Pseudomonas aeruginosa*. Biochemistry 43:5239–5245
242. Uchida T, Sekine Y, Matsui T, Ikeda-Saito M, Ishimori K (2012) A heme degradation enzyme, HutZ, from *Vibrio cholerae*. Chem Commun 48:6741–6743

243. Lad L, Schuller DJ, Shimizu H, Friedman J, Li H, Ortiz de Montellano PR, Poulos TL (2003) Comparison of the heme-free and -bound crystal structures of human heme oxygenase-1. J Biol Chem 278:7834–7843
244. Schuller DJ, Wilks A, Ortiz de Montellano PR, Poulos TL (1999) Crystal structure of human heme oxygenase-1. Nat Struct Mol Biol 6:860–867
245. Unno M, Matsui T, Ikeda-Saito M (2012) Crystallographic studies of heme oxygenase complexed with an unstable reaction intermediate, verdoheme. J Inorg Biochem 113:102–109
246. Lad L, Ortiz de Montellano PR, Poulos TL (2004) Crystal structures of ferrous and ferrous–NO forms of verdoheme in a complex with human heme oxygenase-1: catalytic implications for heme cleavage. J Inorg Biochem 98:1686–1695
247. Sugishima M, Sakamoto H, Higashimoto Y, Noguchi M, Fukuyama K (2003) Crystal structure of rat heme oxygenase-1 in complex with biliverdin-iron chelate. Conformational change of the distal helix during the heme cleavage reaction. J Biol Chem 278:32352–32358
248. Lad L, Friedman J, Li H, Bhaskar B, Ortiz de Montellano PR, Poulos TL (2004) Crystal structure of human heme oxygenase-1 in a complex with biliverdin. Biochemistry 43:3793–3801
249. Sharma PK, Kevorkiants R, de Visser SP, Kumar D, Shaik S (2004) Porphyrin traps its terminator! Concerted and stepwise porphyrin degradation mechanisms induced by heme-oxygenase and cytochrome P450. Angew Chem Int Ed 43:1129–1132
250. Kumar D, de Visser SP, Shaik S (2005) Theory favors a stepwise mechanism of porphyrin degradation by a ferric hydroperoxide model of the active species of heme oxygenase. J Am Chem Soc 127:8204–8213
251. Chen H, Moreau Y, Derat E, Shaik S (2008) Quantum mechanical/molecular mechanical study of mechanisms of heme degradation by the enzyme heme oxygenase: the strategic function of the water cluster. J Am Chem Soc 130:1953–1965
252. Matsui T, Nakajima A, Fujii H, Mansfield Matera K, Migita CT, Yoshida T, Ikeda-Saito M (2005) O_2- and H_2O_2-dependent verdoheme degradation by heme oxygenase. Reaction mechanisms and potential physiological roles of the dual pathway degradation. J Biol Chem 280:36833–36840
253. Lai W, Chen H, Matsui T, Omori K, Unno M, Ikeda-Saito M, Shaik S (2010) Enzymatic ring-opening mechanism of verdoheme by the heme oxygenase: a combined X-ray crystallography and QM/MM study. J Am Chem Soc 132:12960–12970
254. Damaso CO, Bunce RA, Barybin MV, Wilks A, Rivera M (2005) The ferrous verdoheme–heme oxygenase complex is six-coordinate and low-spin. J Am Chem Soc 127:17582–17583
255. Gohya T, Sato M, Zhang X, Migita CT (2008) Variation of the oxidation state of verdoheme in the heme oxygenase reaction. Biochem Biophys Res Commun 376:293–298
256. Zhou H, Migita CT, Sato M, Sun D, Zhang X, Ikeda-Saito M, Fujii H, Yoshida T (2000) Participation of carboxylate amino acid side chain in regiospecific oxidation of heme by heme oxygenase. J Am Chem Soc 122:8311–8312
257. Zeng Y, Deshmukh R, Caignan GA, Bunce RA, Rivera M, Wilks A (2004) Mixed regioselectivity in the Arg-177 mutants of *Corynebacterium diphtheriae* heme oxygenase as a consequence of in-plane heme disorder. Biochemistry 43:5222–5238
258. Lad L, Wang J, Li H, Friedman J, Bhaskar B, Ortiz de Montellano PR, Poulos TL (2003) Crystal structures of the ferric, ferrous and ferrous-NO forms of the Asp140Ala mutant of human heme oxygenase-1: catalytic implications. J Mol Biol 330:527–538
259. Ratliff M, Zhu W, Desmukh R, Wilks A, Stojiljkovic I (2001) Homologues of neisserial heme oxygenase in gram-negative bacteria: degradation of heme by the product of the *pigA* gene of *Pseudomonas aeruginosa*. J Bacteriol 183:6394–6403

260. Caignan GA, Deshmukh R, Wilks A, Zeng Y, Huang H, Moënne-Loccoz P, Bunce RA, Eastman MA, Rivera M (2002) Oxidation of heme to β- and δ-biliverdin by *Pseudomonas aeruginosa* heme oxygenase as a consequence of an unusual seating of the heme. J Am Chem Soc 124:14879–14892
261. Deshmukh R, Zeng Y, Furci LM, Huang H, Morgan BN, Sander S, Alontaga AY, Bunce RA, Moënne-Loccoz P, Rivera M, Wilks A (2005) Heme oxidation in a chimeric protein of the α-selective *Neisseriae meningitidis* heme oxygenase with the distal helix of the δ-selective *Pseudomonas aeruginosa*. Biochemistry 44:13713–13723
262. Peng D, Ma L-H, Smith KM, Zhang X, Sato M, La Mar GN (2012) Role of propionates in substrate binding to heme oxygenase from *Neisseria meningitidis*: a nuclear magnetic resonance study. Biochemistry 51:7054–7063
263. Zhang X, Fujii H, Mansfield Matera K, Migita CT, Sun D, Sato M, Ikeda-Saito M, Yoshida T (2003) Stereoselectivity of each of the three steps of the heme oxygenase reaction: hemin to meso-hydroxyhemin, meso-hydroxyhemin to verdoheme, and verdoheme to biliverdin. Biochemistry 42:7418–7426
264. Torpey J, Ortiz de Montellano PR (1996) Oxidation of the *meso*-methylmesoheme regioisomers by heme oxygenase. Electronic control of the reaction regiospecificity. J Biol Chem 271:26067–26073
265. Evans JP, Niemevz F, Buldain G, Ortiz de Montellano PR (2008) Isoporphyrin intermediate in heme oxygenase catalysis. Oxidation of α-meso-phenylheme. J Biol Chem 283:19530–19539
266. Torpey J, Ortiz de Montellano PR (1997) Oxidation of α-*meso*-formylmesoheme by heme oxygenase. Electronic control of the reaction regiospecificity. J Biol Chem 272:22008–22014
267. Lemberg R, Legge JW, Lockwood WH (1939) Coupled oxidation of ascorbic acid and haemoglobin. I. Biochem J 33:754–758
268. Avila L, Huang H, Damaso CO, Lu S, Moënne-Loccoz P, Rivera M (2003) Coupled oxidation vs heme oxygenation: insights from axial ligand mutants of mitochondrial cytochrome b5. J Am Chem Soc 125:4103–4110
269. O'Carra P (1975)) Heme cleavage: biological systems and chemical analogs. In: Smith KM (ed) Porphyrins and metalloporphyrins. Elsevier, Amsterdam, pp 123–153 (Chapter 4)
270. Brown SB, Docherty JC (1978) Haem degradation in abnormal haemoglobins. Biochem J 173:985–987
271. Murakami T, Morishima I, Matsui T, Ozaki S, Hara I, Yang H-J, Watanabe Y (1999) Effects of the arrangement of a distal catalytic residue on regioselectivity and reactivity in the coupled oxidation of sperm whale myoglobin mutants. J Am Chem Soc 121:2007–2011
272. Vernon DI, Brown SB (1984) Formation of bile pigments by coupled oxidation of cobalt-substituted haemoglobin and myoglobin. Biochem J 223:205–209
273. Rice JK, Fearnley IM, Barker PD (1999) Coupled oxidation of heme covalently attached to cytochrome b_{562} yields a novel biliprotein. Biochemistry 38:16847–16856
274. Avila L, Huang H, Rodríguez JC, Moënne-Loccoz P, Rivera M (2000) Oxygen activation by axial ligand mutants of mitochondrial cytochrome b5: oxidation of heme to verdoheme and biliverdin. J Am Chem Soc 122:7618–7619
275. Kräutler B (2003)) Chlorophyll breakdown and chlorophyll catabolites. In: Kadish KM, Smith KM, Guilard R (eds) The porphyrin handbook, vol 13. Academic, San Diego, pp 183–209 (Chapter 82)
276. Masuda T, Fujita Y (2008) Regulation and evolution of chlorophyll metabolism. Photochem Photobiol Sci 7:1131–1149
277. Moser S, Müller T, Oberhuber M, Kräutler B (2009) Chlorophyll catabolites – chemical and structural footprints of a fascinating biological phenomenon. Eur J Org Chem 21–31
278. Barry CS (2009) The stay-green revolution: recent progress in deciphering the mechanisms of chlorophyll degradation in higher plants. Plant Sci 176:325–333

279. Hörtensteiner S, Wüthrich KL, Matile P, Ongania K-H, Kräutler B (1998) The key step in chlorophyll breakdown in higher plants. Cleavage of pheophorbide a macrocycle by a monooxygenase. J Biol Chem 273:15335–15339
280. Pružinská A, Tanner G, Anders I, Roca M, Hörtensteiner S (2003) Chlorophyll breakdown: pheophorbide *a* oxygenase is a Rieske-type iron–sulfur protein encoded by the accelerated cell death 1 gene. Proc Natl Acad Sci USA 100:15259–15264
281. Troxler RF, Smith KM, Brown SB (1980) Mechanism of photo-oxidation of bacteriochlorophyll-*c* derivatives. Tetrahedron Lett 21:491–494
282. Iturraspe J, Gossauer A (1991) Dependence of the regioselectivity of photo-oxidative ring opening of the chlorophyll macrocycle on the complexed metal ion. Helv Chim Acta 74:1713–1717
283. Okamoto Y, Tamiaki H (2011) C3- and C13-substituent effects on electronic absorption spectra of linear tetrapyrroles produced by photooxidation of zinc chlorophyll derivatives. J Photochem Photobiol A Chem 219:250–254
284. Saito S, Furukawa K, Osuka A (2010) Fully π-conjugated helices from oxidative cleavage of *meso*-aryl-substituted expanded porphyrins. J Am Chem Soc 132:2128–2129
285. Berlicka A, Latos-Grażyński L, Szterenberg L, Pawlicki M (2010) Photooxidation of dithiaethyneporphyrin. Eur J Org Chem 5688–5695
286. Pawlicki M, Bykowski D, Szterenberg L, Latos-Grazyński L (2012) From 21,23-dioxaporphyrin to a 3-pyranone dioxacorrole skeleton: the Achmatowicz rearrangement in the porphyrin frame. Angew Chem Int Ed 51:2500–2504